The separation of the Cerenkov light and particle fronts in extensive air showers at sea level

Shearer, J. A. L.

THE SEPARATION OF THE CERENKOV LIGHT AND PARTICLE FRONTS IN EXTENSIVE AIR SHOWERS AT SEA LEVEL

by

J.A.L. Shearer, B.Sc.

A Thesis submitted to the University of Durham in accordance with the Regulations for Admittance to the Degree of Master of Science

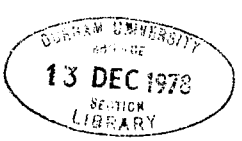

Department of Physics
University of Durham

JUNE 1978

ABSTRACT

This thesis describes a study of the separation of Cerenkov light and particle fronts in large cosmic ray air showers. The work was carried out during the winters of 1975/76 and 1976/77 at the British Universities Joint Air Shower array at Haverah Park.

A description of the work to date on Cerenkov light in air showers is given to complement the study. A theoretical treatment, based on computer simulations, of the separation is given as well as the experimental results obtained during the two seasons.

A description of a more advanced experiment studying Cerenkov light in E.A.S. is also presented. The experimental work described was the responsibility of the author.

CONTENTS

- CHAPTER ONE -

The Cosmic Radiation

1.1 Introduction

Mankind receives information about the observable universe via a number of mechanisms; most, however comes from studies of the electromagnetic spectrum. Information carried by this means is indirect, as theories have to be elaborated to relate the observed radiation with conditions at source. However, the matter contained in what have become known as the cosmic rays can be regarded as the only presently available means of studying material which has originated outside the solar system.

The cosmic radiation consists of energetic nuclei, electrons and gamma rays. It covers a large gamut of energies from 10^9 eV (below this energy particles can be considered to be local phenomena) to energies in excess of 10^{20}eV. Wilson in 1901 first noticed that there existed a background of highly penetrating radiation, but was unable to identify its source. It remainded for Heiss (1912) to show that the radiation was of extra-terrestial origin. Early work on the radiation concentrated on studying the physical nature of the particles and their interactions at high energies. Many of the fundamental steps in understanding the behaviour of particles have come from cosmic ray studies; this is particularly so in the case of the meson, which owes most of its theoretical and experimental development to cosmic ray studies. Since the advent of accelerators much of the work previously carried out by studies of the radiation can be achieved under controlled conditions; consequently, in recent years more attention has been devoted to the astrophysical aspects of the radiation.

From an astrophysical view point the interest in the radiation can be divided into three categories:-

(I) the energy spectrum of the radiation

(II) the mass spectrum of the radiation

(III) sites of origin of the radiation

The observed energy spectrum is shown in figure 1-1 , two important features can be noted; these are changes in slope at $\approx 10^{16}$ and 10^{19} eV. These changes have been interpreted as indicating at 10^{16} eV a decrease in intensity due to diffusion of the particles with lower charge out of the galaxy and at 10^{19} eV with contributions from extra-galactic particles becoming dominant. Greisen (1966) indicated that if the extragalactic particles had a sufficient path length then interactions with the 2.7 K background would become important. Hillas (1975) discussed the effect of other universal mechanisms which would reduce the intensity of the highest energetic particles. Hillas also indicated that above 5.10^{19} eV the energy spectrum should steepen dramatically. This effect has not yet been observed, but the apparent flattening of the spectrum at these energies appears to be contrary to these expectations. If this flattening can be verified then it either severely limits the possible sites of origin of the radiation or has strong implications for present cosmological models.

Due to the isotropic nature of the cosmic radiation no distinct sources can be seen. The isotropy is thought to result from the interactions between the charged particles and the galactic magnetic field. The particles will spiral in the field with a radius of curvature much less than the expected source distance; typically 1 parsec and 100 parsec respectively. However, at low energies, $E_p < 10^{12}$ eV, solar modulation effects have been observed, indicating a solar origin for some of the particles at this energy. At this energy, as well, there have been indications of a focusing of the radiation down the local spiral arm, indicative of a galactic origin of the radiation. At

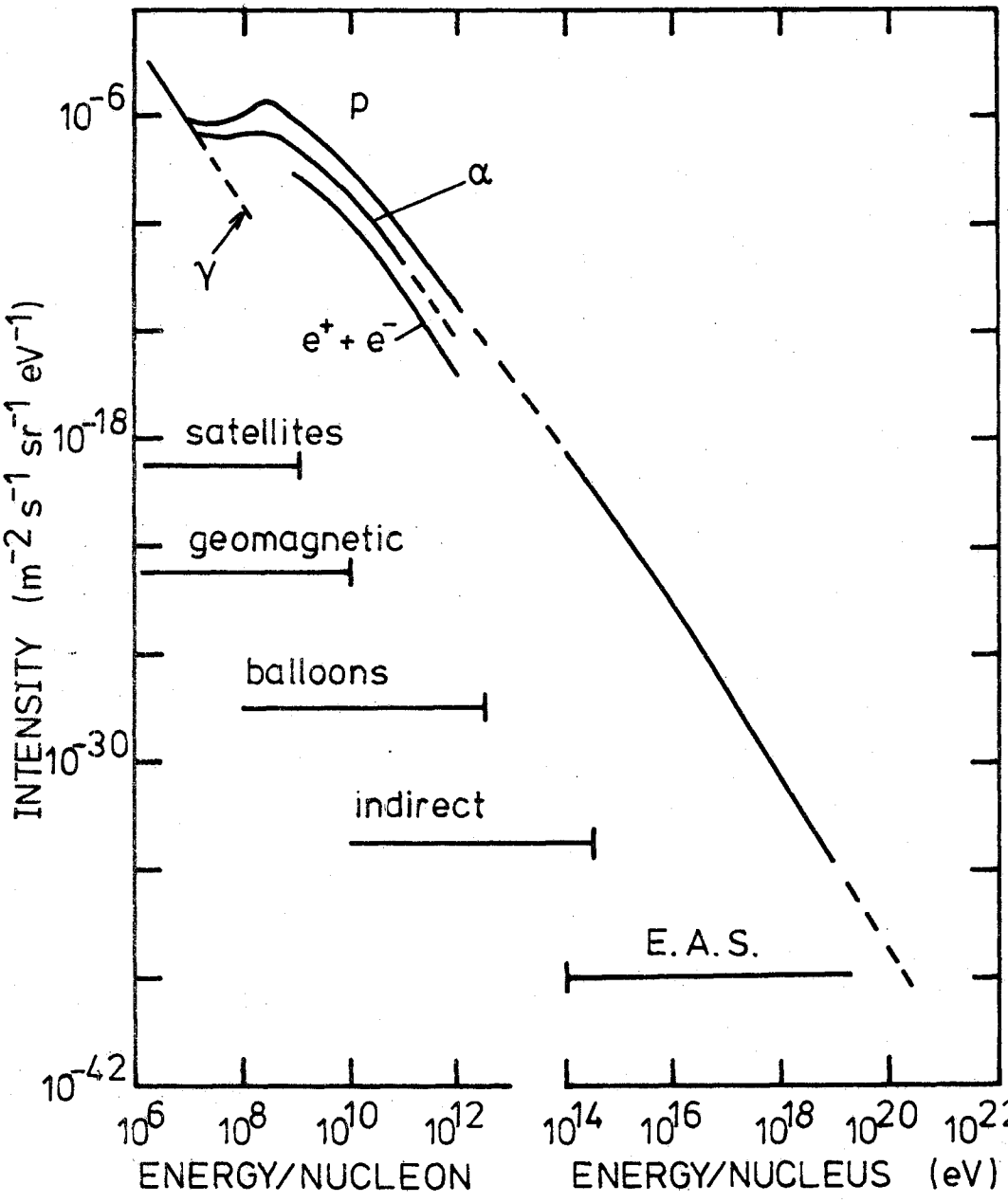
p
α
γ
e⁺ + e⁻
satellites
geomagnetic
balloons
indirect
E.A.S.
INTENSITY (m⁻² s⁻¹ sr⁻¹ eV⁻¹)
10⁻⁶
10⁻¹⁸
10⁻³⁰
10⁻⁴²
10⁶ 10⁸ 10¹⁰ 10¹²
ENERGY/NUCLEON
10¹⁴ 10¹⁶ 10¹⁸ 10²⁰ 10²²
ENERGY/NUCLEUS (eV)

the very highest energies, $E_p > 10^{18}$ eV, statistics are beginning to emerge which show a certain anistropy, probably caused by the enhanced contribution of extragalactic particles. Thus although no complete picture of the origins has been established, observations are beginning to indicate, not necessarily individual sites but regions where the radiation is likely to have originated.

1.2 Extensive Air Showers

The steepness of the primary energy spectrum, see figure 1-1 , means that the particles of the highest energy have an extremely low flux; e.g. the flux at 10^{16} eV is 1 m^{-2}/2 years compared to 1 m^{-2}/3000 years at 10^{18} eV. It can be seen that without recourse to excessive patience or cost the primary beam cannot be observed directly at these energies. However the atmosphere presents itself as an absorber of thickness 1030 gm /cm^2, which is large compared to, say, the mean free path of a proton. Consequently, the primary will interact several times with air nuclei before reaching ground level. The secondary particles and their progeny produced by these interactions make up an extensive air shower (EAS) which can be observed over a large area.

Accelerator studies indicate that after a primary - air nucleus collision the majority of particles produced will be pi - mesons. After the initial interaction the primary will continue with about half its energy and collide again to produce more pions, and so on. The charged pions produced will either interact with air nuclei to produce more pions or will decay to muons which survive to the observational plane. The neutral pions produced will decay almost instantaneously to two gamma rays which produce an electron - positron pair which via bremsstrahulung create more photons and so an electromagnetic cascade develops. This cascade is continually replenished by the hadronic cascade following the primary through the atmosphere. Although in terms of number of particles the

electromagetic cascade is the largest it only carries 10% of the total energy of the shower. The most energetic component is the hadronic cascade. The electron and muon component of an EAS have a wide lateral spread and can be detected over 1 kilometre from the passage of the primary. This allows for the use of widely spaced detectors to overcome the problem of a low flux at high energies. By sampling the the distribution of particles at ground level it is possible to obtain information about the primary. The majority of the world's arrays use this technique, of sampling, to construct the ground level situation in a shower; the normal means of detection being the scintillation light produced in either liquid or plastic scintillators. There are exceptions, the most notable deviation away from the normal situation being the deep water tanks at Haverah Park. These detectors observe the Cerenkov light produced by the passage of a charged particle through tanks of 1 metre thickness containing clear water. The cheapness of these tanks facilitiates the use of large detecting areas. In the core of a shower, hodoscopes, cloud chambers and flash tubes have been employed to study the hadronic cascade. This sort of study is only feasible for the low energy showers as the cascade has to pass directly through the detector, an unlikely occurence at high energies. Techniques have been developed by which observations of e.g. the radio emission or scintillation light from the electronic cascade can be used to give direct evidence of the structure of the electronic cascade, without recourse to extrapolation from ground level. One of these techniques, Cerenkov emission, will be described in greater depth in the next chapter.

1.3 The Mass Spectrum of the Primary Beam

At low energies (E_p less than 10^{12} eV) the distribution of masses has been accurately measured by studying the passage of the primary

through nuclear emulsion stacks flown in balloons. The observed mass spectrum is shown in Table 1-1 from two experiments. The comparison figures show that the cosmic ray beam at these energies is enriched with 'heavy' nuclei, when compared to the universal abundance distribution. At energies higher than these it becomes increasingly difficult to measure the mass directly and no firm estimate has been made. It is at these energies, however, that the mass spectrum becomes increasingly important as it strongly relates to the problem of determining an origin for the radiation. If it is to be assumed that the radiation up to 10^{18} eV is of galactic origin, then it would be expected that particles of low charge would diffuse out of the galaxy sooner than those of higher charge. Thus the beam at high energies would be expected to be enriched in heavy nuclei. This tendency has been observed by Juliusson (1975) for energies up to 10^{13} eV/nucleon. If it can be shown that the beam is of uniform composition then it places severe limits on the sources of the particles and on the structure and strength of the galactic magnetic field. Above 10^{19} eV it is difficult to imagine anything other than a purely protonic beam of extragalactic origin, as the acceleration and propogation processes would preclude heavier material, and sufficient mechanisms cannot be found, at present, within the galaxy to account for the high energy.

If the tendencies observed at lower energies were extrapolated to the air shower region, then it can be seen that the majority of the cosmic rays in the region 10^{16} to 10^{18} eV would consist of the iron peak elements. Figure 1-2 shows the energy spectrum from 10^{10} to 10^{20} eV, showing the contribution from various element groups, Figure 1-3 shows an interpretation of this distribution, after Juliusson (1975). This author interprets the beam composition to be purely iron from 10^{16} eV, the position of the 'knee' in the energy spectrum. When the 'ankle' at 10^{19} eV is considered then it appears that Juliusson's analysis requires

Table 1-1

energy	total no. of events	% protons and neutrons	% of α particles	% of heavier particles	reference
3.7×10^{11}	46	80	13	7	Malhotra et al (1966)
$> 10^{12}$	112	46	16	38	Mc Cusker (1967)
universal composition	——	≈ 99	< 1	$< .02$	——

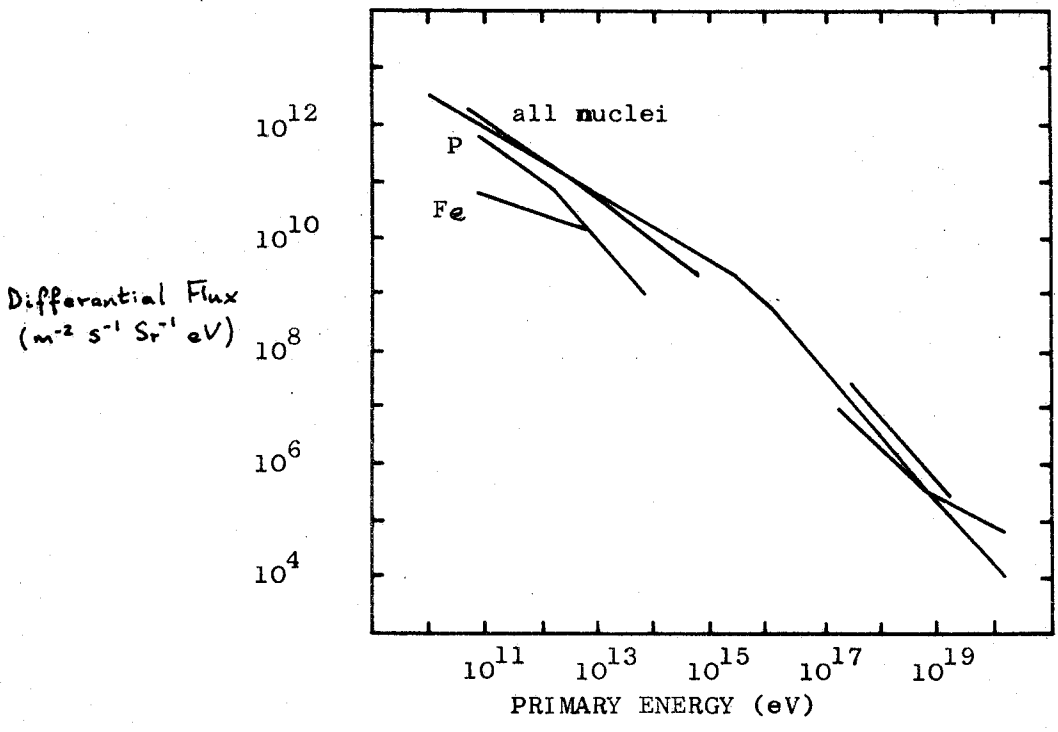
Differantial Flux
(m⁻² s⁻¹ Sr⁻¹ eV)
10¹²
10¹⁰
10⁸
10⁶
10⁴
all nuclei
P
Fe
10¹¹
10¹³
10¹⁵
10¹⁷
10¹⁹
PRIMARY ENERGY (eV)

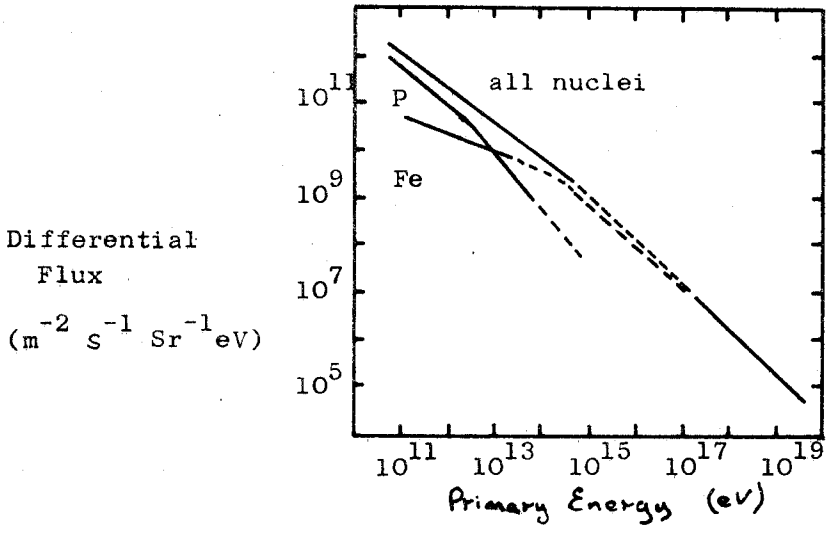
Differential
Flux
(m⁻² s⁻¹ Sr⁻¹ eV)
10¹¹
10⁹
10⁷
10⁵
all nuclei
P
Fe
10¹¹
10¹³
10¹⁵
10¹⁷
10¹⁹
Primary Energy (eV)

modification to account for the expected extragalactic contribution. The existence of this 'ankle' requires further work to establish it unequivocably and until the mass at air shower energies has been measured none of these speculations can be justified.

1.4 This work

It is the aim of this thesis to give a description of the recent work which has been carried out on the Cerenkov light emitted by air showers. A detailed description of a potentially useful parameter, the separation of the Cerenkov light front and the particle front, is given. It is hoped that this parameter may be used to complement other studies relating to identifying the mass of the primary beam. Chapter 2 reviews the work which has been carried out on Cerenkov radiation from large air showers.

Chapters 3 & 4 provides an experimental and theoretical treatment of the delay between the Cerenkov light and particle fronts in extensive air showers.

Chapter 5 discusses the future studies of the light to be carried out by the Durham University group.

- CHAPTER TWO -

Cerenkov Light in Extensive Air Showers

2.1 Introduction

It was first suggested by Blackett (1948) that Cerenkov radiation emitted by cosmic ray particles in the atmosphere would make a significant contribution to the general night sky brightness. Galbraith and Jelley (1953) tested this proposal for the general enhancement by considering the situation during an EAS when a large number of particles are available to radiate over a short period of time (10's of nanoseconds). Thus, if a receiver with a short time constant is used, during an EAS it is possible to consider the night sky brightness as a static source, with the Cerenkov contribution being temporarily increased. In their experiment the authors used a photomultiplier with a simple optical arrangement, which was placed at the centre of an array of Geiger - Muller tubes. They noticed a coincidence on 22 out of 50 occasions between the photomultiplier signal and the discharge of one or two of the Geiger - Muller tubes. A series of later studies by the same authors, Galbraith and Jelley (1955), at the Pic du Midi Observatory produced indications of the origin of the radiation; namely that it was polarised and had a spectrum consistent with Cerenkov radiation. Nesterova and Chudakov (1955) produced similar conclusions from a program of work in the Soviet Union.

2.2 Theoretical Considerations

2.2.1 Preamble

Before describing recent results of computer simulations of the radiation from large showers, it is necessary to consider why the origin of the light is to be expected to be a Cerenkov mechanism rather than other mechanisms. Most of the discussion which follows is taken from the reviews of Cerenkov light by Boley (1964) and Jelley (1967).

If the case of one electron is considered, the expected energy loss E per unit path length h due to the Cerenkov effect for electrons of velocity v between λ and $d\lambda$ has been given by Frank and Tamm (1937)

$$\frac{dE}{dh} = 4\pi^2 z^2 \int \left(1 - \frac{1}{\beta^2 n^2}\right) \frac{d\lambda}{\lambda^3} \qquad \text{Equation 2.1}$$

Assuming the refractice index, n, is constant over the region of atmosphere considered here by integrating over $4000 < \lambda < 7000$ Å, for high energy electrons this reduces to:

$$\frac{dE}{dh} = 3.8 \cdot 10^{-9} \mu \text{ erg/cm} \qquad \text{Equation 2.2}$$

where $\mu = \eta - 1$, which assuming no variation with altitude gives, from Boley (1964), 8.2×10^3 photons/radiation length. Therefore for each electron reaching ground level there will be about 10^5 photons produced. This approximate calculation, which is a slight over-estimate indicates the large amplification produced by the Cerenkov effect. If other mechanisms for light production are considered, then Table 2-1 from Jelley (1967) shows clearly how Cerenkov dominates over alternative production mechanisms. The exception is recombination light; a new experiment described by Bergeson (1975) is at present under construction to use this light for a study of the highest energy cosmic rays.

Having shown that Cerenkov light can be produced in sufficient quantities during an EAS to be observed, it becomes necessary to consider whether other forms of light from the night sky could effect any proposed observations. Firstly the continuum radiation from the night sky, which peaks towards the red end of the spectrum (showing an increase in flux six-fold from 3500 Å to 6500 Å). The Cerenkov radiation has, from equation 2.1, an inverse square relationship with increasing wavelength, so the spectrum of the light will peak towards the blue. Thus the night sky although limiting the dynamic range of a

TABLE 2-1 Radiation Processes

For air at STP and radiation in the region 4000-6000 Å (From Jelley (1967))

Process	Assumptions	Angular Distribution	Energy loss $dw/dl(eVcm^{-1})$
Cerenkov	$E_e \lessapprox 100$ MeV	$\sim 1.3^o$	≈ 0.8
Ionization +Recombination	Lifetime of the states $< 5.10^{-8}$ sec	Istotropic	8.10^{-3}
Synchroton	$E_e \lessapprox 3.10^{10}$ eV $E_e \lessapprox 10^9$ eV	In Vacuo(Mc^2/E) In Air 1.3^o	1.3×10^{-7} $\lessapprox e^{-50}$
Bremsstrahlung	$Z = 9$ $E_e = 100$ MeV	Same as for Synchrotron radiation	$< 4.10^{-5}$

proposed experiment does not severely interfere with the detection of Cerenkov light.

Allen (1955) gives the transmission of light through the atmosphere, which increases from 63% at 4000 Å to 83% at 5000 Å. Again although limiting an experiment these figures indicate that the atmosphere will not catastrophically effect the radiation. A detailed description of the effect of aerosol attenuation and Rayleigh scattering can be found in Elterman (1968); these effects are sufficient to require inclusion in any simulation of the radiation. Jelley (1967) discusses the effect of dispersion, diffraction and refraction and he concludes that they do not significantly effect the Cerenkov light produced in the atmosphere.

The conclusion Jelley arrives at concerning the effect of dispersion, diffraction and refraction is important in the context of large EAS. The mean angle of emission of Cerenkov light has been shown by Jelley to be 1.3^{o} so the light retains information about the direction of the emitting electron. If this direction can be maintained throughout the atmosphere, then the lateral ground spread of the light at ground level can be related to the lateral spread of the electrons higher in the atmosphere. This maintenance of directionality will be shown in section 2.4 to have important consequences for studies of the longitudinal cascade.

2.2.2 Simulations of Cerenkov Light

It is the intention in this section to outline the simulations of Cerenkov light, as well as indicating that parameters of ground based observations can be utilised in studies of the physical nature of the primary particle. It is not the intention to describe in detail the validity of any model used in the presented simulation results, since it is intended that parameters can be found which are effectively model independent.

In any study of the cosmic radiation it is vital to have a means whereby ground based observations can be interpreted in terms of the nature of the primary. It is with this aim in view that simulations of EAS have been carried out where the progeny of the initial interaction have been followed down through the atmosphere, thereby creating a picture of the expected ground based situation. The Cerenkov light emitted during an EAS is inexcorably linked to the electron-photon cascade, so it is this cascade and how it relates to the general development of an EAS that is of importance in Cerenkov light studies. The following parameters and their relation to the general development of an EAS will be considered:

I) the lateral spread of the light

II) the pulse profiles

III) the shape of the light front

a) The lateral spread

Considering the unique relation of Cerenkov light to the longitudinal cascade of the electrons arising from the fact that the observed photon flux is the integral, over a detectors angle of view, of the complete cascade. It is therefore to be expected that the integral over all core distances of this photon flux is related to the total number of electrons and hence the primary energy. Dyakanov et al (1973) have shown that the Cerenkov light flux is effectively independent of model and depends, almost linearly, on the primary energy, Figure 2-1 . Data from Protheroe and Turver (1977) show however the expected flattening of the light distribution resulting from the differing depths of initial interaction caused by considering the average cascades of proton, alpha and iron nuclei primaries. In measurements at Haverah Park the photon density at 200 metres, Ø (200), has been found to be an adequate primary energy estimator. Figure 2-2 shows an early

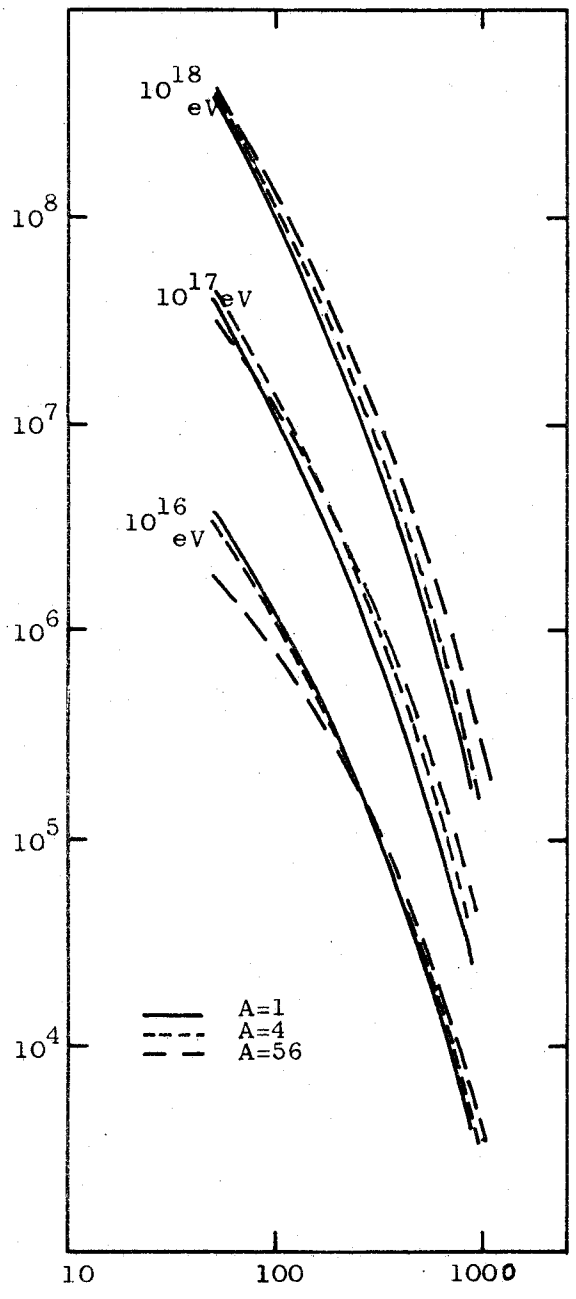
10^{18} eV
10^{17} eV
10^{16} eV
10^8
10^7
10^6
10^5
10^4
A=1
A=4
A=56
10
100
1000
Photon density (m^{-2})
Core distance (m)

calculation for the expected lateral distribution for proton initiated showers at various energies; Figure 2-3 shows the lateral distribution for a sample of showers at 10^{17} eV, both from Smith and Turver (1973). From these two figures it can be seen that at a core distance of about 200 metres the photon density is virtually independent of cascade development and only relates to primary energy (for energies $\leq 10^{17}$ eV).

b) Pulse Profiles

Boley (1964) first suggested that the temporal structures of the light signal contained information on the electron cascade development.

Kalymkov et al (1975) have suggested that the FWHM of a Cerenkov pulse is related to the depth of maximum. This result has been extended by Protheroe and Turver (1977) to include other temporal characteristics of Cerenkov pulses. By considering the electron cascade in terms of eight individual sub-showers and then by using the Cerenkov light emitted by these sub-showers, the origin of the pulse shape may be established. Figure 2-4 shows the electron cascade and its individual components, indicating the height of origin of the individual showers, Figure 2-5 shows the resultant lateral distributions. Figure 2-6 shows how the ground level Cerenkov pulses are constructed from the sub-showers. At core distances $r > 150$ metres it can be seen that the Cerenkov pulse maps directly the electron cascade. Consequently, the rise time of the pulse reflects the situation around the start of the cascade, the FWHM the situation about maximum, and the fall time the decay of the shower. The experimental consequences of this are discussed in section 2.4.

c) The Shape of the Light Front

The early experimental work on Cerenkov light indicated that the first light originated at an altitude of about 2 km , see e.g. Boley (1961) and Bradley and Porter (1960). This appears to be in contrast with the expectations from calculations mentioned above; however, when it is considered that these results came from measurements made at close core

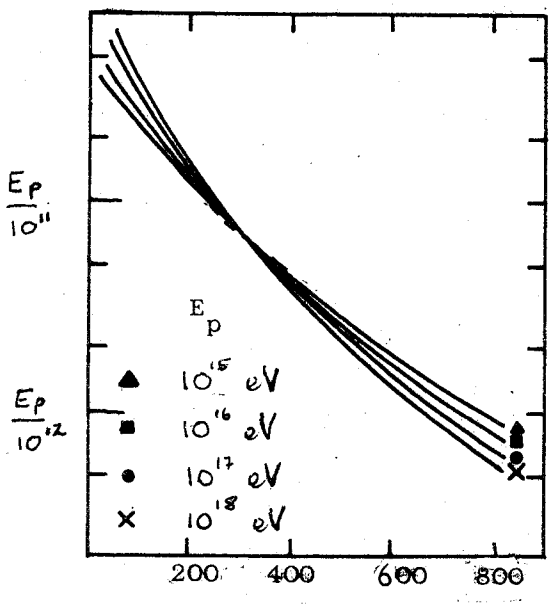

Photon Density m^{-2}

Core Distance (m)

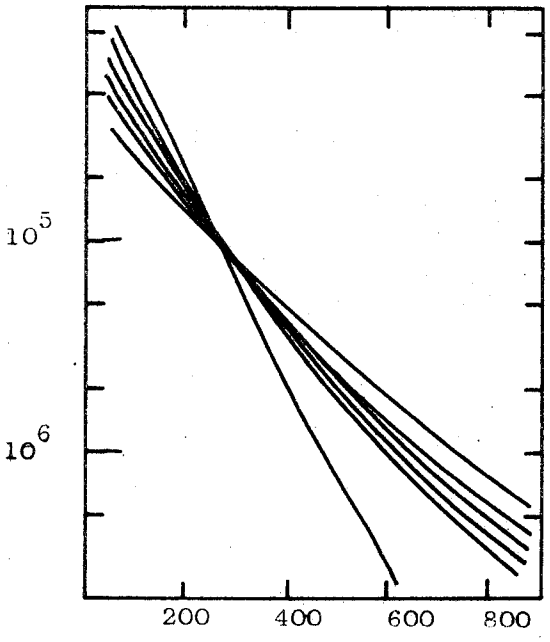

Photon Density m^{-2}

Core Distance (m)

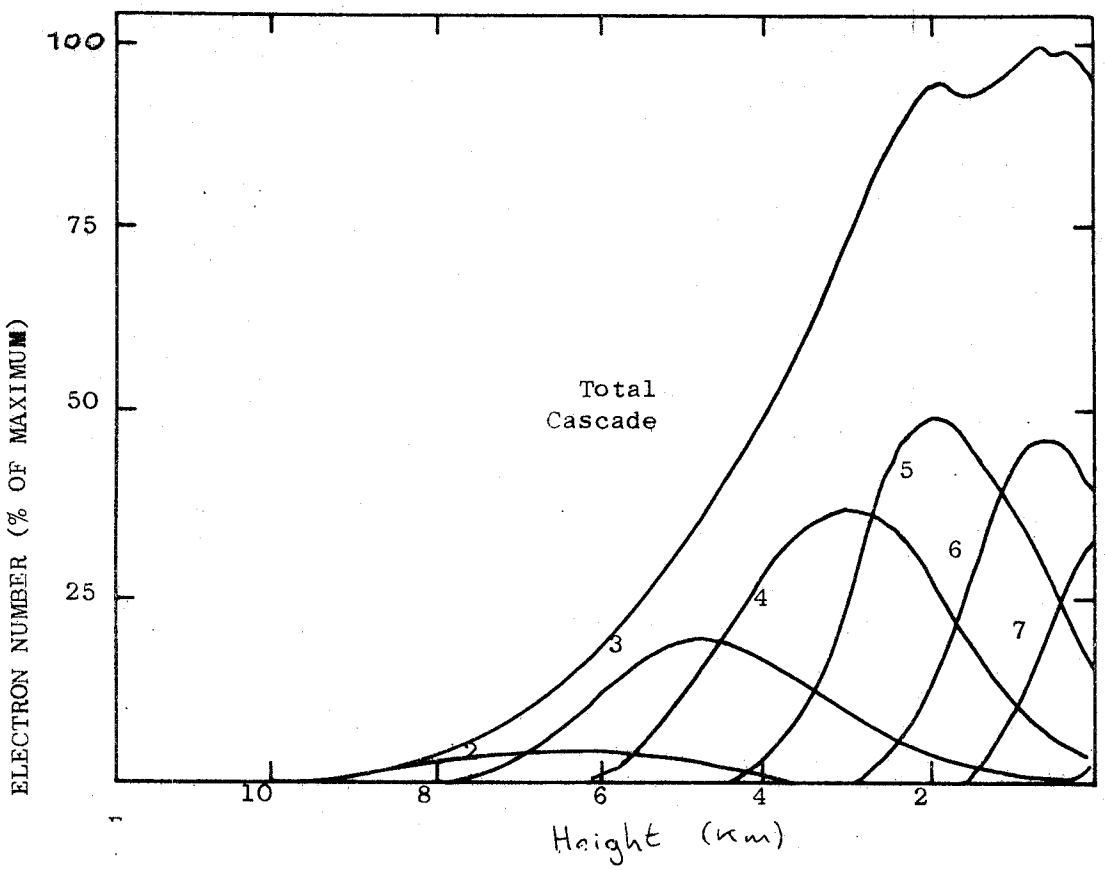
100
75
50
25
ELECTRON NUMBER (% OF MAXIMUM)
Total
Cascade
2
3
4
5
6
7
10
8
6
4
2
Height (km)

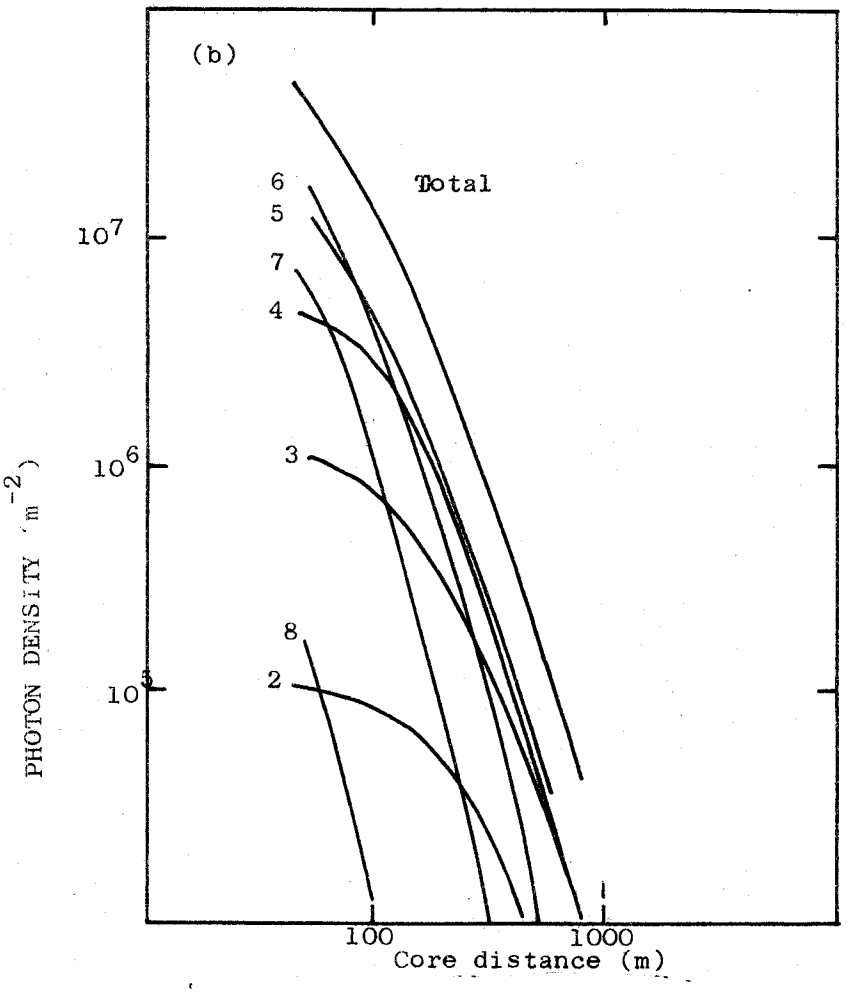
(b)
Total
6
5
7
4
3
8
2
10^7
10^6
10^5
PHOTON DENSITY (m^{-2})
100
1000
Core distance (m)

distances, $r \lesssim 50$ metres, where it is expected that the light would be local in origin. Figure 2-7 shows fits for a spherical front at various levels through a pulse. It is clear from the curvature of the 10% point that the first light originates high in the atmosphere, also that the fits for the various other levels confirm the suggestion that the light in the Cerenkov pulse maps the longitudinal cascade of the electrons. The justification for choosing a spherical front can be seen from the small deviation from the calculated points.

2.2.3 Summary

The simulation results have highlighted which shower parameters can be effectively used to describe the development of an EAS. We expect that the primary energy can be estimated to within 20% by measuring the light flux at 200 metres. It has also been shown that the pulse shape parameters reflect the development of the electronic cascade, thus emphasising the possibility of being able to measure certain parameters within the longitudinal cascade. This is of great importance to studies of the mass spectrum of the primary beam. Although no parameter relates directly to the mass of the primary it is hoped that by considering the shower as a whole that it will be possible to identify the mass; see for example Dixon (1974), who considered the feasibility of mass identification using cluster analysis.

2.3 Measurements of Cerenkov Radiation

The unique relationship between the Cerenkov light and the longitudinal cascade have already given rise to studies to identify the mass of the primary beam using Cerenkov light. However, no experiment has yet been able to identify the mass independently of the model for the high energy interactions used in the analysis. Kreiger and Bradt (1971), for example, concluded from their experiment that the beam around 10^{16} eV is of mixed

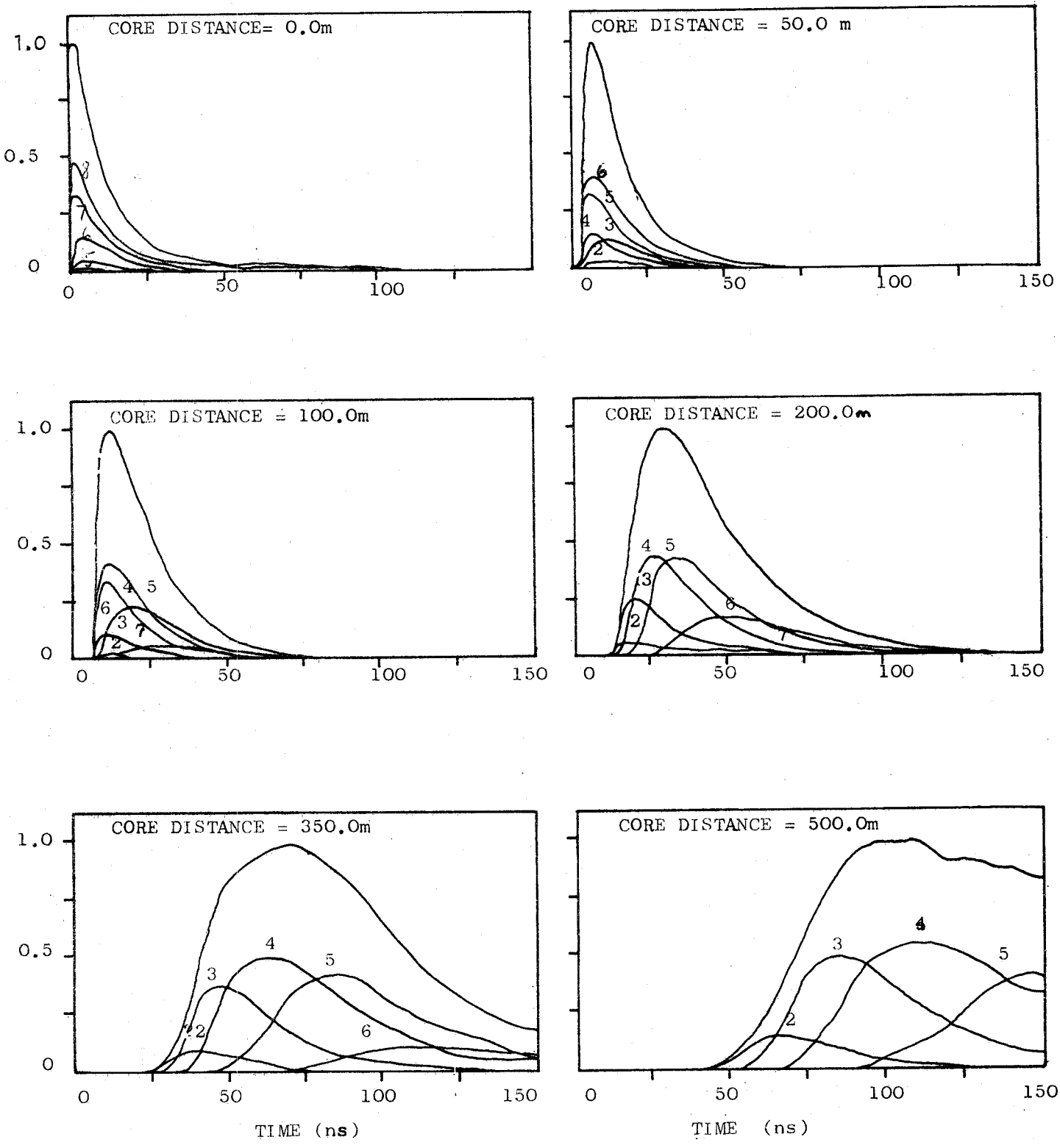
CORE DISTANCE= 0.Om
CORE DISTANCE = 50.0 m
CORE DISTANCE = 100.Om
CORE DISTANCE = 200.Om
CORE DISTANCE = 350.Om
CORE DISTANCE = 500.Om
1.0
0.5
0
0
50
100
150
TIME (ns)

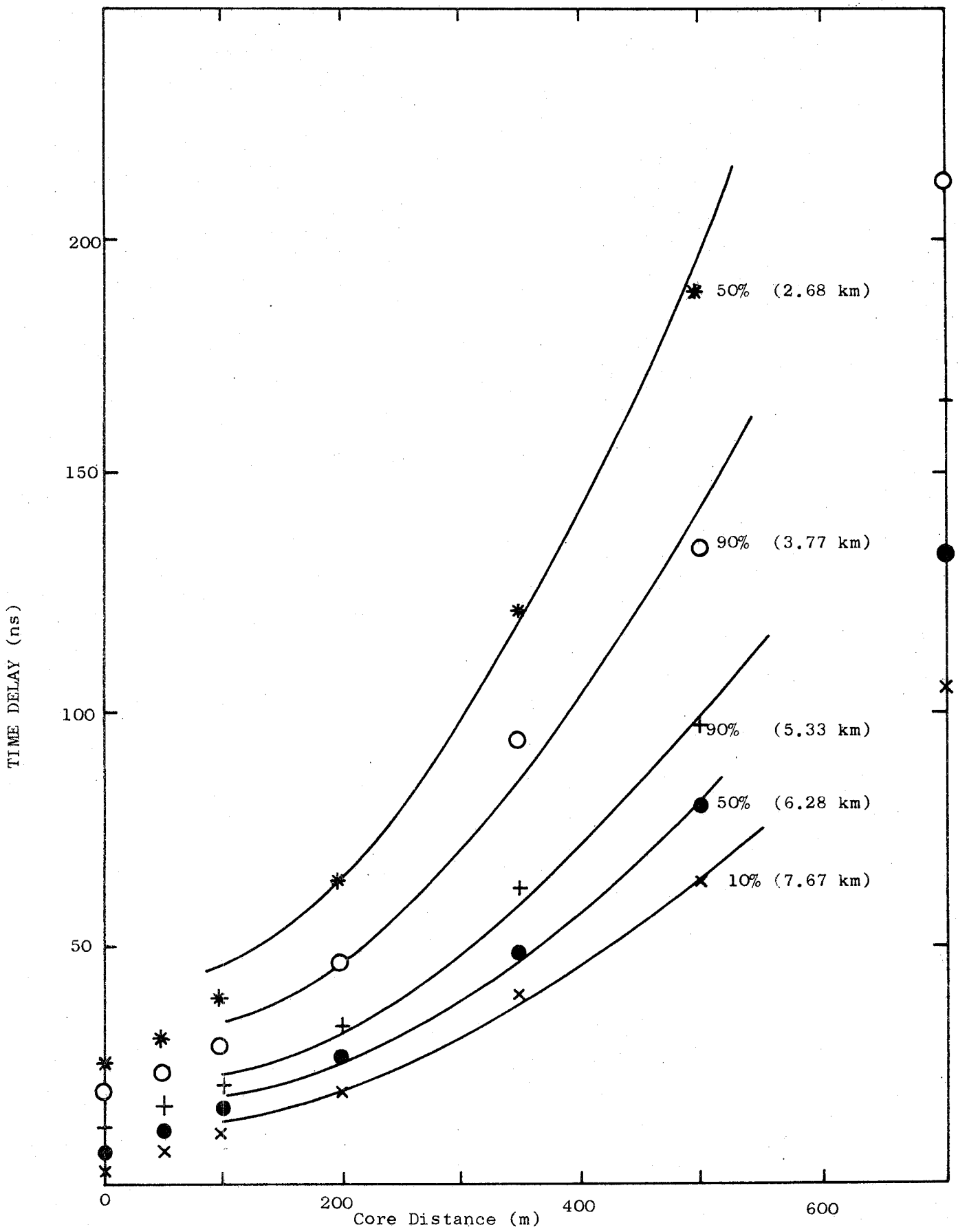
TIME DELAY (ns)
200
150
100
50
0
200
400
600
Core Distance (m)
50% (2.68 km)
90% (3.77 km)
90% (5.33 km)
50% (6.28 km)
10% (7.67 km)

composition. However, they also indicate that their results could be interpreted in terms of a purely protonic beam, 10% of which interacts with the atmosphere with an inelasticity of unity. The problem of choosing a model is highlighted by comparing the CKP and scaling model, Cocconi et al (1961) and Feynman (1969) respectively. Figure 2-8 compares the observations of Hammond et al (1978) with those of Kalmykov (1975), indicating also the expectations from simulations for the two different models. (N.B. Hammond et al consider detector response in their calculations.)

At Haverah Park the Durham group has developed an array of 8 photo-multipiers to observe Cerenkov radiation in showers of energy $\gtrsim 10^{17}$eV.

Figure 2-9 shows the geometrical layout of the array, the Cerenkov detectors were, with the exception of the one on hut 12, colocated with the deep water tanks forming the established particle array. The effective bandwidth of the system was 35 MHz, thus allowing some measure of the pulse structure to be retained. Although operating in good weather conditions for only 60 hours during the winter of 1975/76 enough information could be gathered to confirm that Cerenkov light can provide a valuable means of studying fluctuations in shower development.

The array was run in conjunction with the particle array, from which a particle analysis was obtainable for comparison. A detailed account of the operation of the experiment can be found in Wellby (1978), and only a brief account of the main results will be considered here. Figures 2-10, 2-11 and 2-12 show the correlation between rise, top and fall time of the pulse and core distance; also shown are the results of of simulations for $A = 4$ and 56 at a similar energy. Figure 2-13 shows the validity of choosing $\emptyset(200)$ as the primary energy estimator. A preliminarly study of the observed fluctuations was also made. By calibrating the observed quantities in terms of the change in zenith angle,

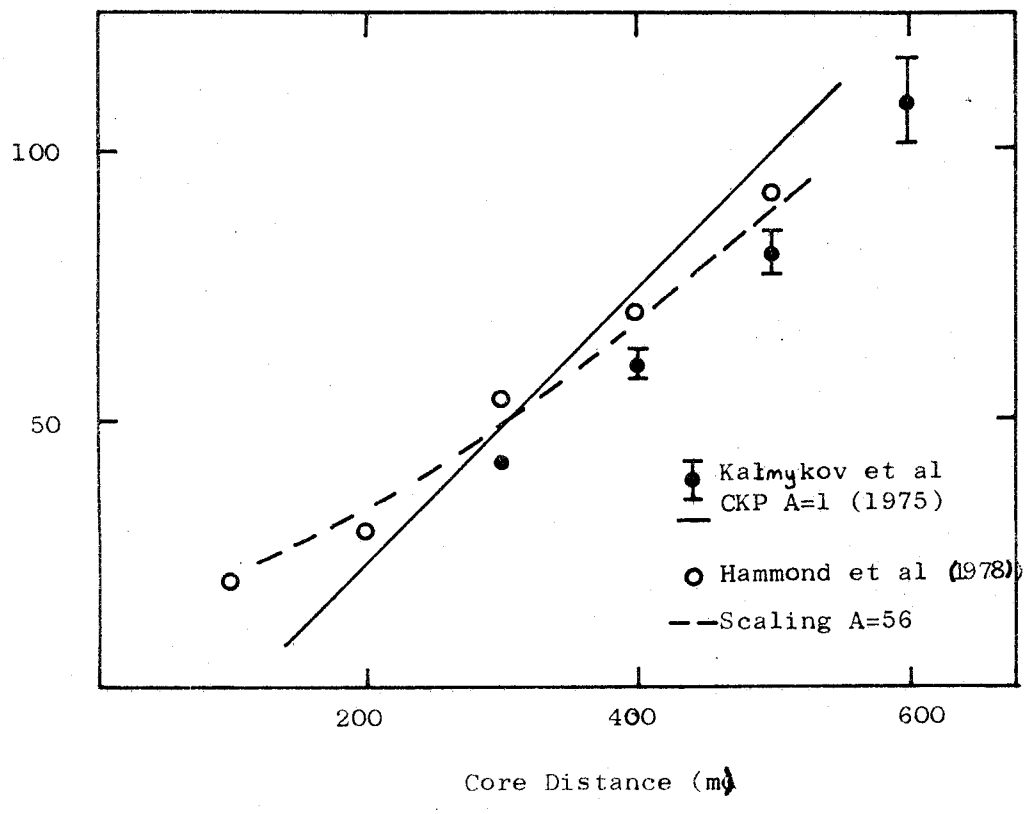
100
50
200
400
600
Kalmykov et al
CKP A=1 (1975)
Hammond et al (1978)
Scaling A=56
Core Distance (m)

WHM
nsec)

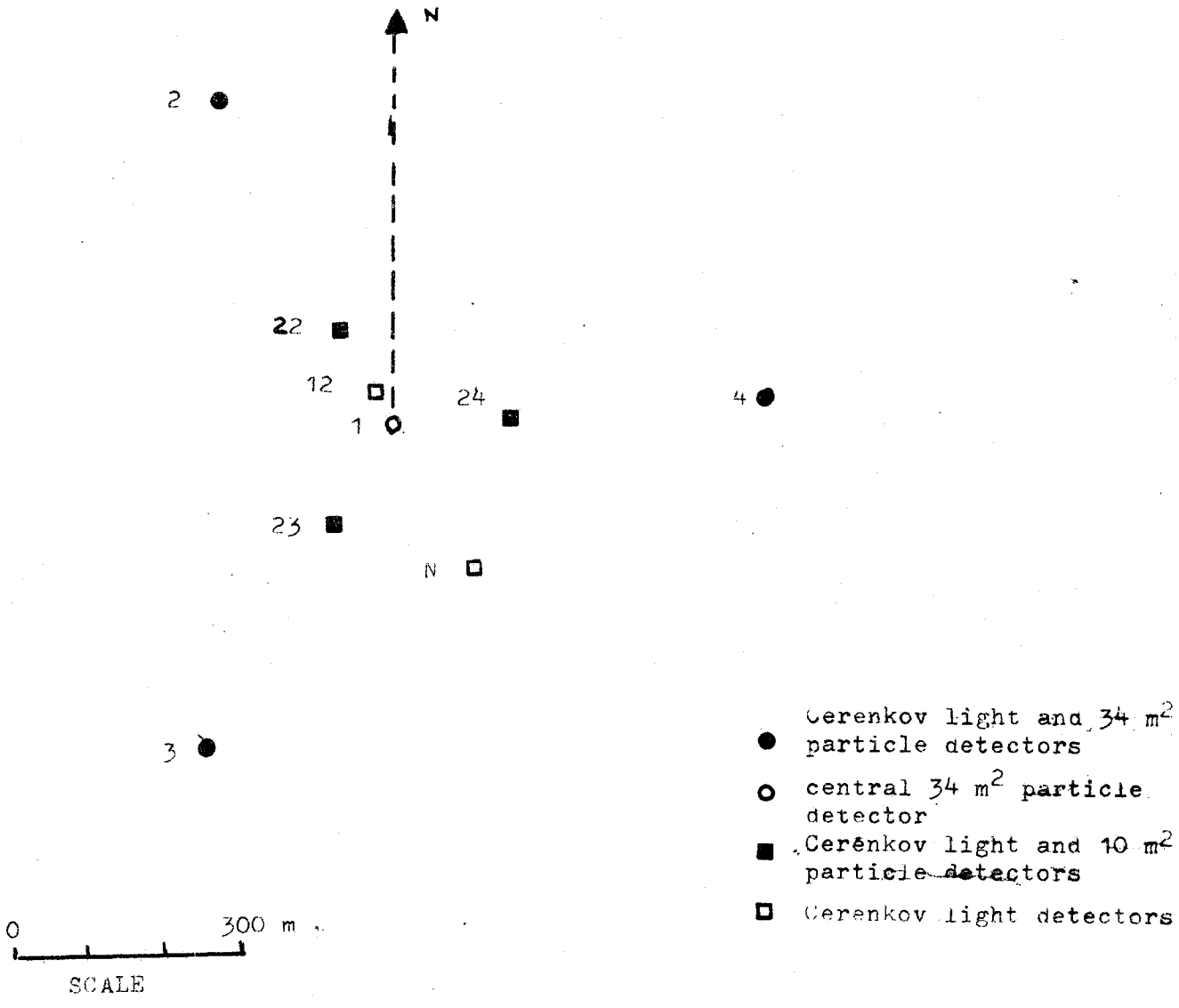
N
2
22
12
1
24
4
23
N
3
0
300 m
SCALE
Cerenkov light and 34 m² particle detectors
central 34 m² particle detector
Cerenkov light and 10 m² particle detectors
Cerenkov light detectors

se time
0% - 90%)
n sec

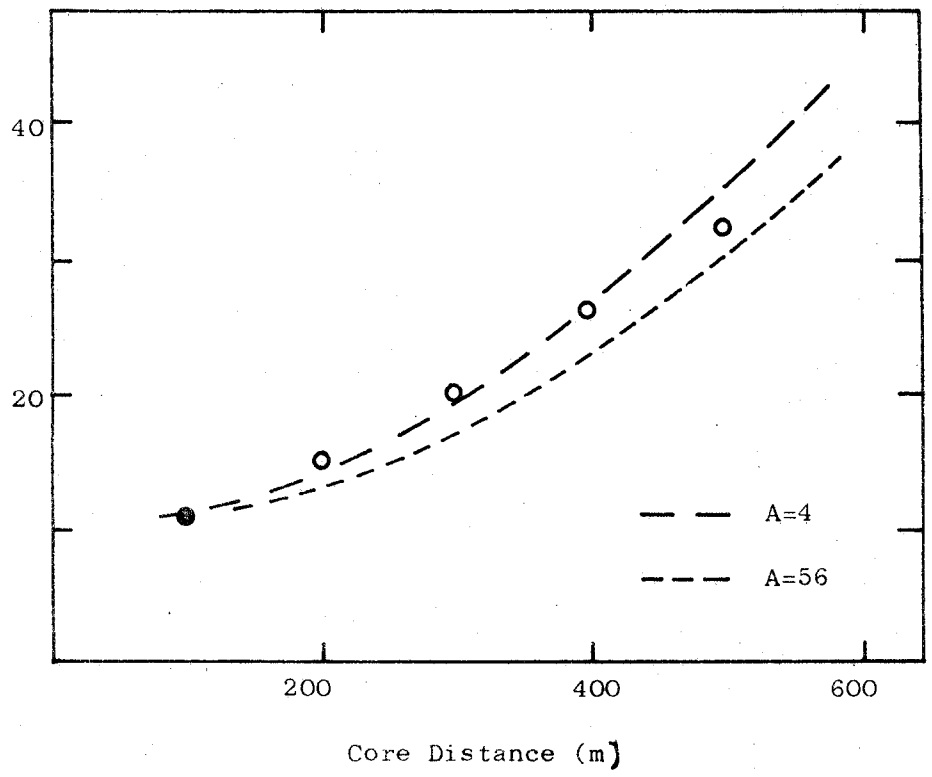

op time
90% - 90%)
nsec

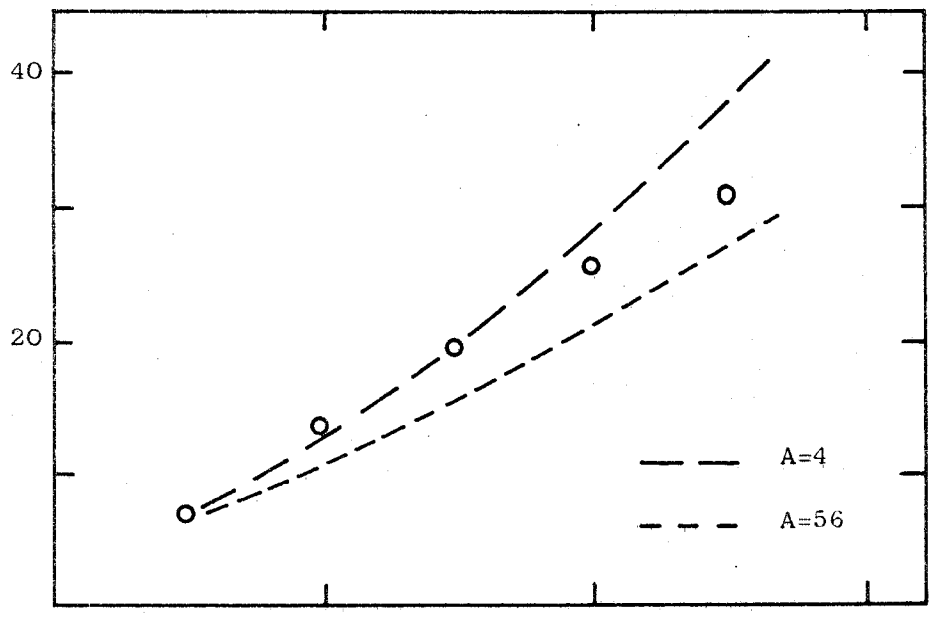

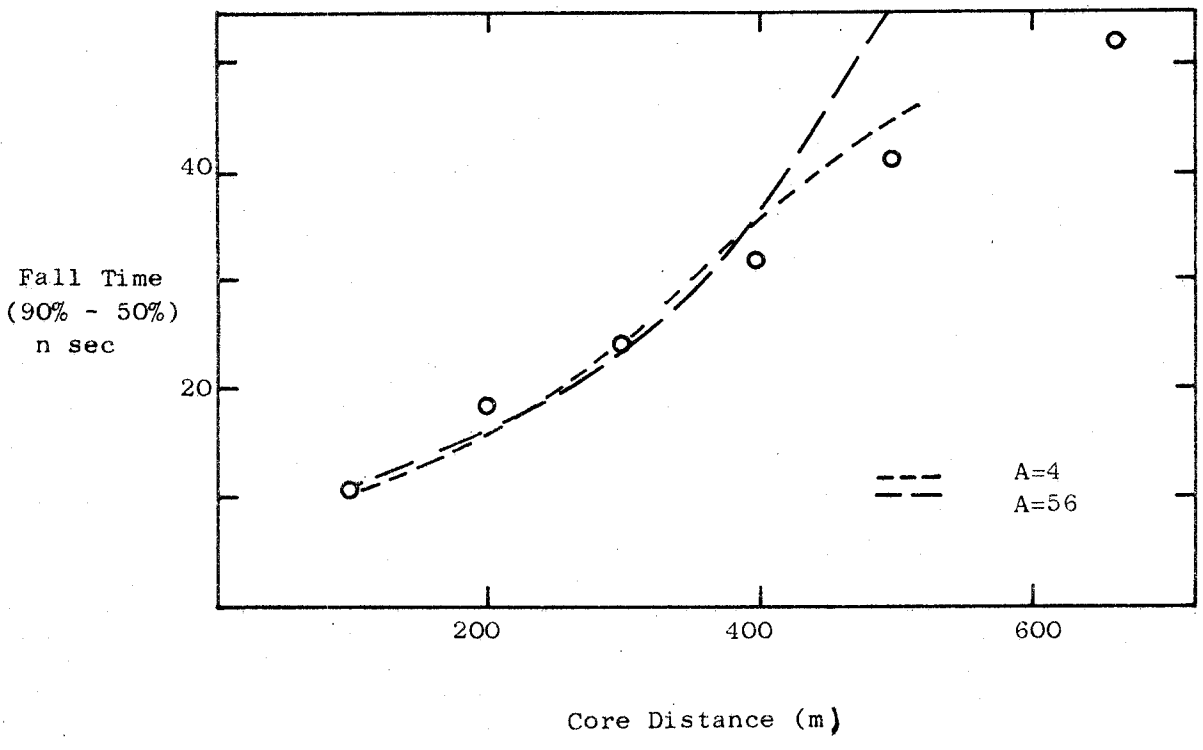
40
20
Fall Time
(90% - 50%)
n sec
200
400
600
A=4
A=56
Core Distance (m)

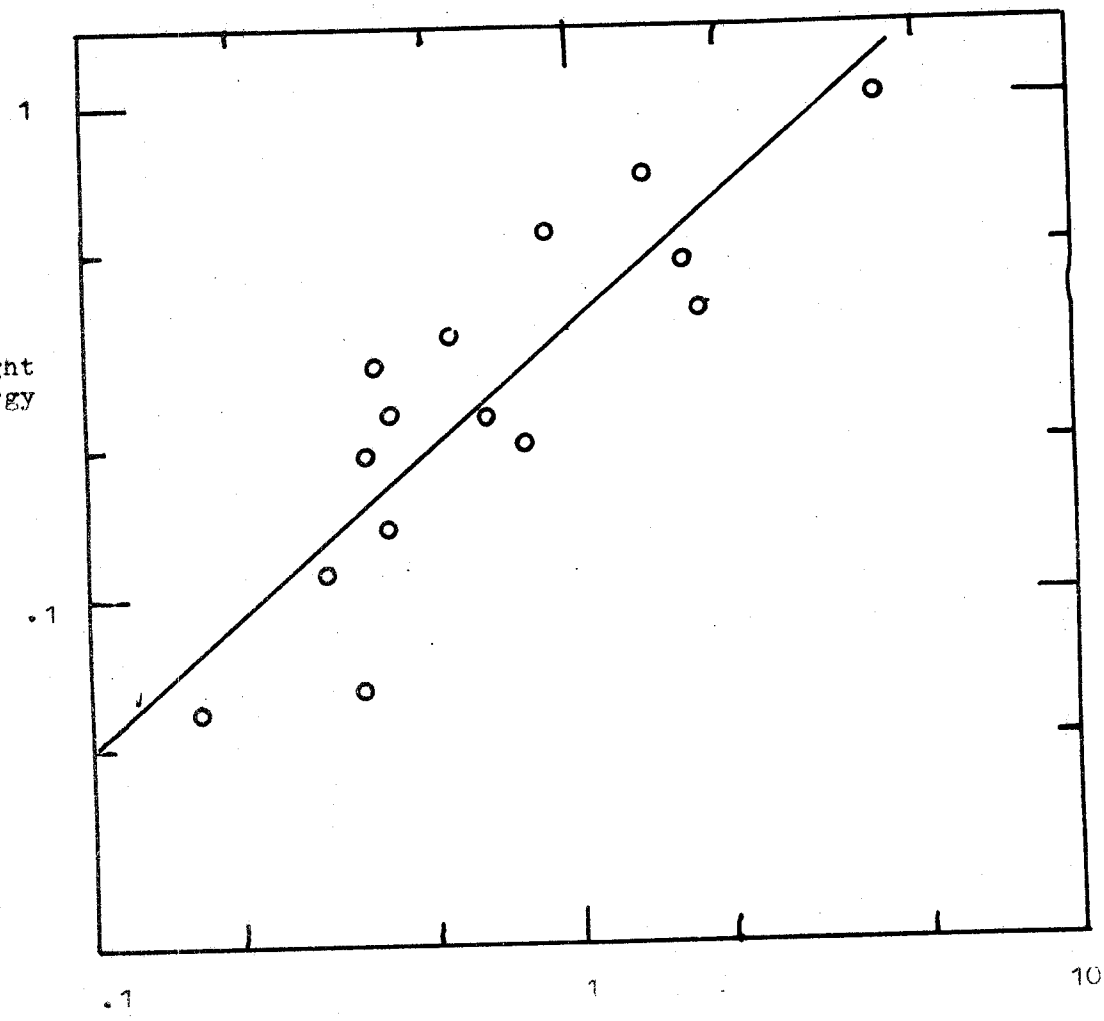

renkov Light
imary Energy
Estimator
ϕ (200)

Particle Array Primary Energy Estimator ρ (500)VE

and primary energy, it was possible to interpret the results to give changes in depth of maximum of individual EAS independently of any model considerations. By this means it was found that the technique was sensitive to changes in development of the order of $\lesssim 100$ g cm^{-2}. Wellby (1978). Unfortunately, due to the sparcity of events, it was not possible to reliably use these results to determine the mass of the primary.

2.4 Analysis of the Temporal Structure of Cerenkov Radiation

Referring to the results described in section 2.2.(b), it was seen that beyond a core distance of 150 metres the Cerenkov pulse shape maps the electronic cascade directly. This facet can be used to obtain direct evidence of the growth of the cascade. For example, the shower front at the 10% level on the rising edge can be regarded as a sphere, whose centre is the region where the shower reaches 10% of its development. This, as figure 2-7 showed, can be extended to the fronts defined by the times of arrival at other levels within a pulse. It is therefore possible to reconstruct a shower in terms of percentage development of the electronic cascade. No measure is made of the absolute electron number at these points, but this can be obtained by calibrating the Cerenkov detectors in terms of an absolute photon flux.

This technique has been described by Orford and Turver (1976) and Hammond et al (1978). It was used to obtain information about the electron cascade directly, see figure 2-14 for the average of measurements during the winter 1975/76; the results of the observing season 1976/77 will be found in Waddoup (1978). One of the benefits of the technique has been the accurate shower arrival directions which have resulted by joining the points inferred in the atmosphere; furthermore, the intersection of this line with the ground is the conventional core.

The technique outlined above hinges on the Cerenkov light from high altitudes arriving before the light emitted lower in the atmosphere

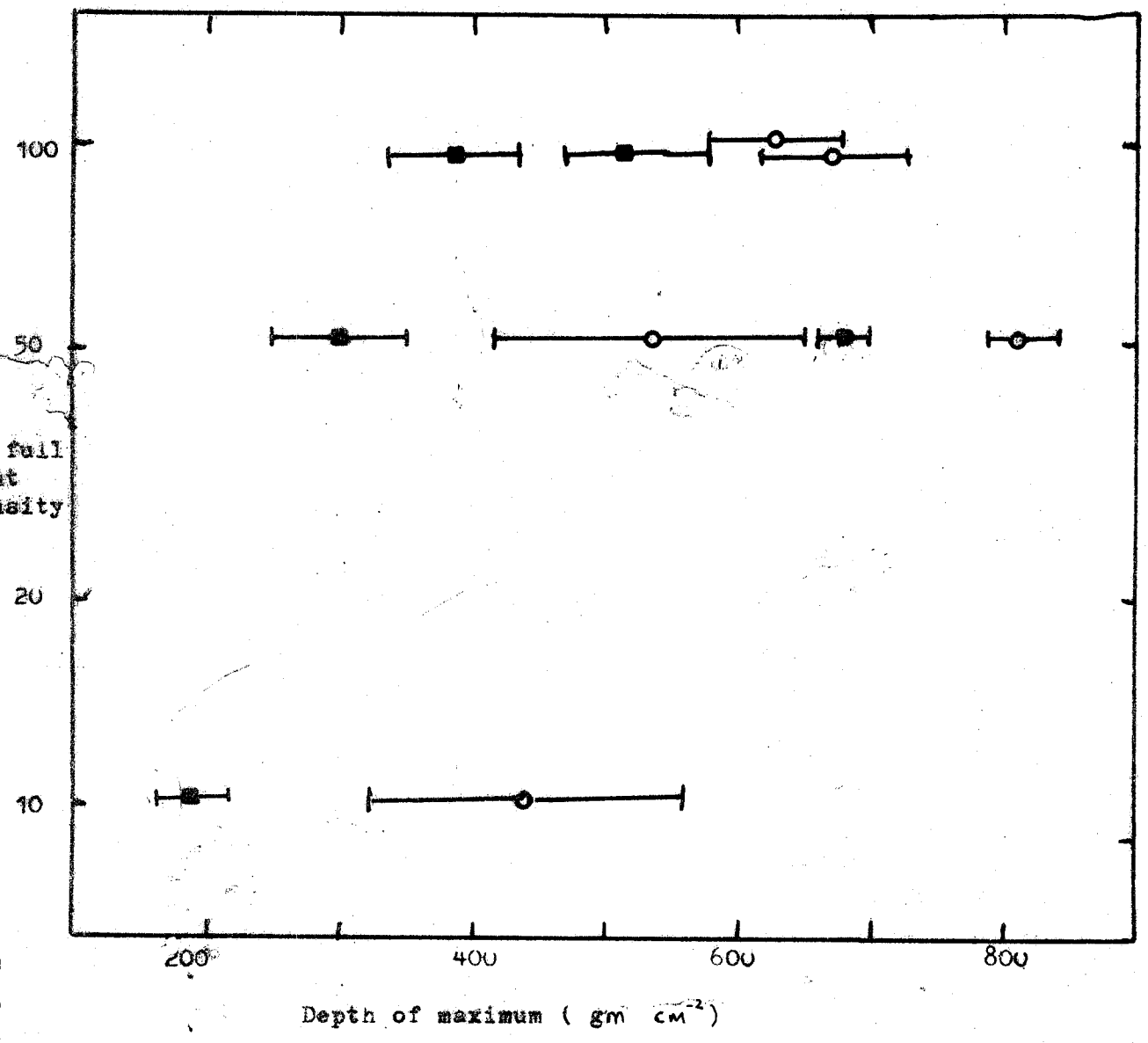
100
50
20
10
200
400
600
800
Depth of maximum (gm cm^{-2})

When the mode of propagation of the electron-photon component is considered it becomes clear that the light at large core distances should arrive before the particles. This could provide a further independent measure of cascade development. Also a direct observation of the delay of the particles behind the light, would confirm the basic assumptions inherent in the above technique. A detailed experimental and theoretical treatment of this delay is discussed in the next two chapters.

- CHAPTER THREE -

The separation of the particle and light fronts

In this chapter the theoretical and experimental nature of the separation between the two fronts is examined. Simple theoretical considerations as well as the results from detailed simulations are considered. The results from preliminary observations made during the winter of 1975/76 are presented.

3.1 Introduction

Following the successful realisation of the technique of relating pulse structure to the structure of the longitudinal cascade, it was thought that, as the technique depended on the first light originating high in the atmosphere, a measurement of the separation between the first light and the first particles may confirm the validity of the assumptions made, as well as supporting the results of recent simulations. Clearly the light and the particles have a common origin, so if it can be shown that the separation of the two fronts increases uniformly with e.g. depth of cascade maximum, then the separation of the two fronts would be an important independent parameter relating to the geometrical distance between the common origin and ground level.

The Cerenkov light will travel at a velocity of c/η, where η is the refractive index of air. The particles causing the light must be travelling in excess of this velocity to produce the radiation. However, if core distances greater than 50 meters are considered, then it has been shown by Hammond et al (1978), that the first light will have originated high in the atmosphere. Considering a photon being emitted from the axis of a shower at a height h and at a time t = 0 and it being detected at ground level at a core distance of r, then the time of detection is given by:

$$t(h,r) = \frac{\sqrt{h^2+r^2}}{c} + \frac{H(\eta_0-1)}{c}\left(1-\exp\left(-\frac{\sqrt{h^2+r^2}}{h}\right)\right)$$

where H is the atmospheric scale height (7.2 km.) and η_0 the refractive index of air at sea level. The first term accounts for path length differences and the second refers to refractive index delays. Figure 3-1 shows this situation graphically for the emission of a photon at 1 km and H kms, it is assumed that the particles causing the emission are travelling between h and 1 km at c. Obviously, if the particles are travelling slower than this then the value of the core distance where the arrival of photons lags behind the particles would be reduced.

If the particles causing the emission of the Cerenkov light high in the atmosphere are to arrive before or coincident with the light at ground level then they must have undergone only small path length delays. In other words the electrons must have a within-pulse timing sequence similar to the Cerenkov light, in that the electrons observed to arrive first must be able to trace their origin directly to the top of the shower. Considering that the atmosphere is about 30 radiation lengths thick then this must mean that the electrons do not undergo scattering sufficient to deviate them significantly away from the passage taken by the light. When it is considered that the $\langle\theta\rangle$ rms for shower electrons is of the order of 12^{o}, then it is untenable to consider that the electrons have not undergone perpendicular as well as transverse motion, before being observed. In essence then the particles will undergo path length delays whilst the light will not, so it is to be expected that the Cerenkov light will arrive before the particles, by an amount related to the core distance of observation and the height at which the light and the electrons can be said to have been coincident.

3.2 Simulations of the separation of the particle and light fronts

In order to extend the simple arguments shown above so that the exact relationship between the separation and conventional shower parameters can be understood, it was necessary to study the results of

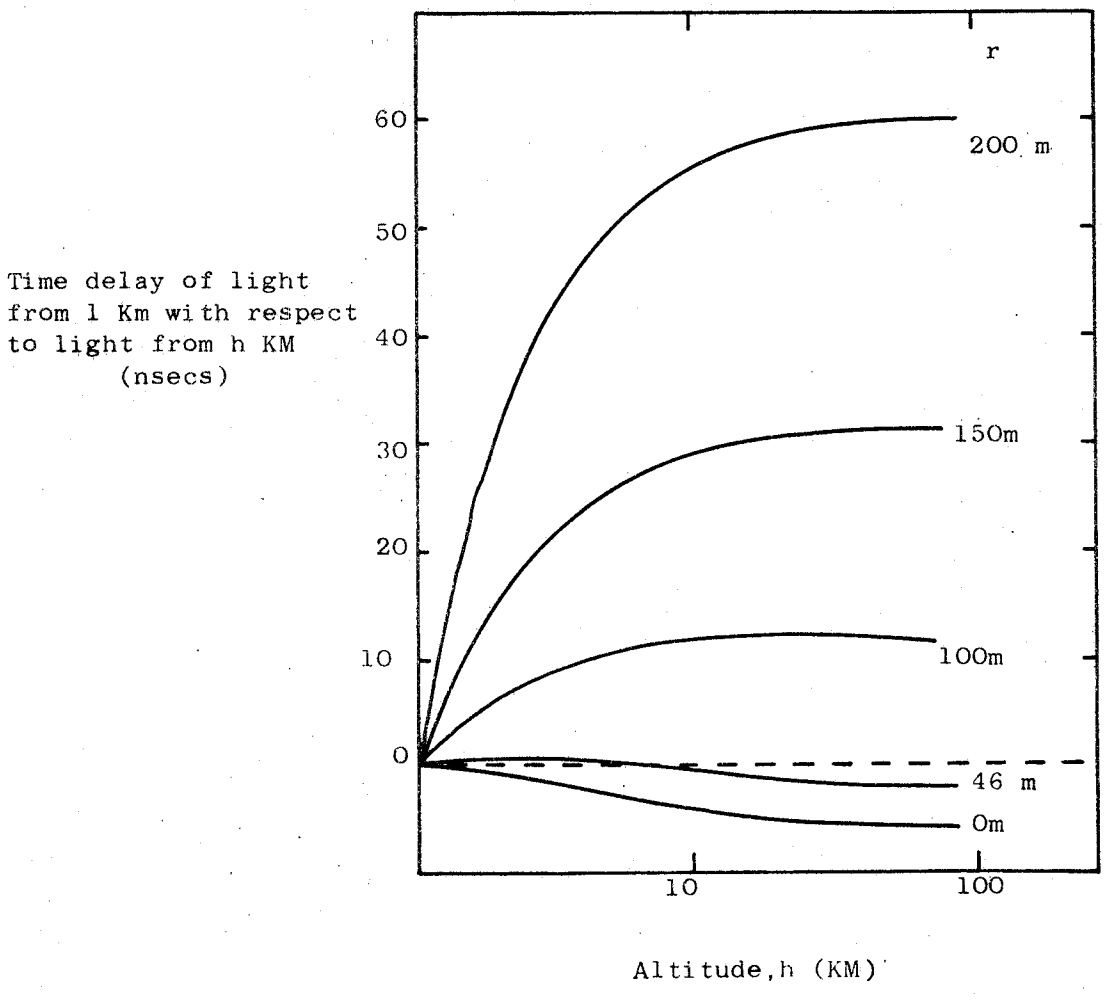
r
60
50
40
30
20
10
0
200 m
150m
100m
46 m
0m
10
100
Time delay of light from 1 Km with respect to light from h KM (nsecs)
Altitude, h (KM)

computer simulations. In this section the results of the work carried out by Protheroe (1978) are discussed. The model for the high energy interaction used in this study was that of scaling and any conclusions reached must be treated as preliminary until confirmation of an acceptable model is made. Where necessary, comparisions between the results from different models are shown.

In order to understand the nature of the delay between the two fronts it is necessary to understand the individual natures of the two fronts. Figure 3-2 shows the expected front for particles arising from a distribution of showers at 5×10^{17} eV and figure 3-3. shows the light front for the same showers. Obviously one factor of importance here is the time at which the front can be said to have arrived. Figure 3-4 shows the effect of setting a lower discrimination threshold for arrival of the particles. Before making comparisions between the fronts it is necessary to decide what the experimental situation will be. As will be shown later measurements were made at Haverah Park during the winter of 1975/76 of the separation between the two fronts at the 10 particle level in deep water detectors and the 10% level on the light signal. So to obtain the delay between the two fronts it is merely a matter of subtracting the two curves shown in figures 3-2 and 3-3. This is shown in figure 3-5. From this it is possible to obtain more understanding of the shape of the function. The light front is essentially spherical with an origin within the region defining the 10% growth point in the shower. The particle front however is flatter and cannot be simply defined in terms of a simple sphere with a particular origin within the shower. Its front arises from a complex sum of all the contributions to the particle density coming from various points within the shower. To discover the effect of various shower parameters on the separation of the two fronts the effect of these parameters on the two individual fronts has to be considered.

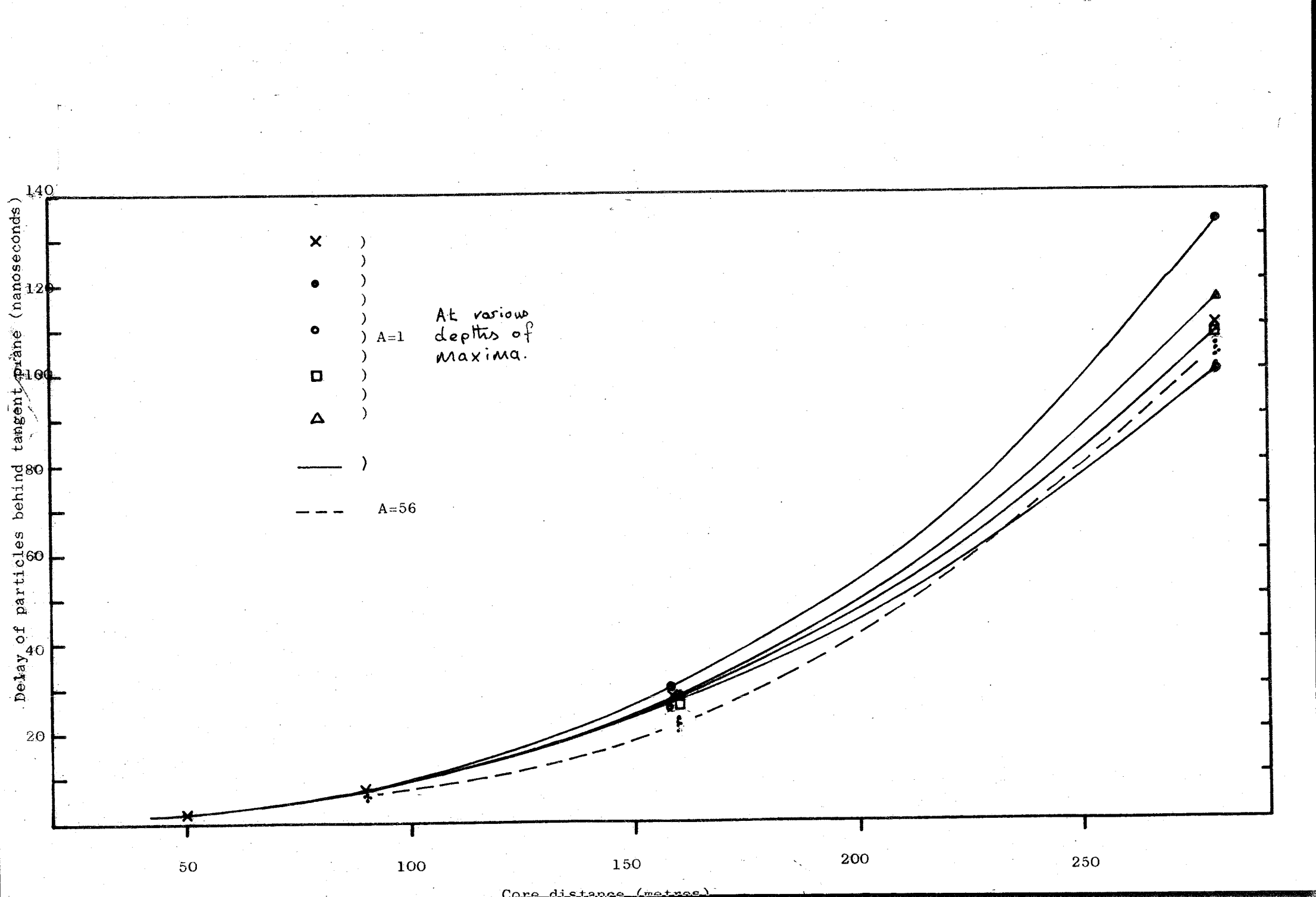
140
120
100
80
60
40
20
Delay of particles behind tangent plane (nanoseconds)
A=1
At various depths of maxima.
A=56
50
100
150
200
250
Core distance (metres)

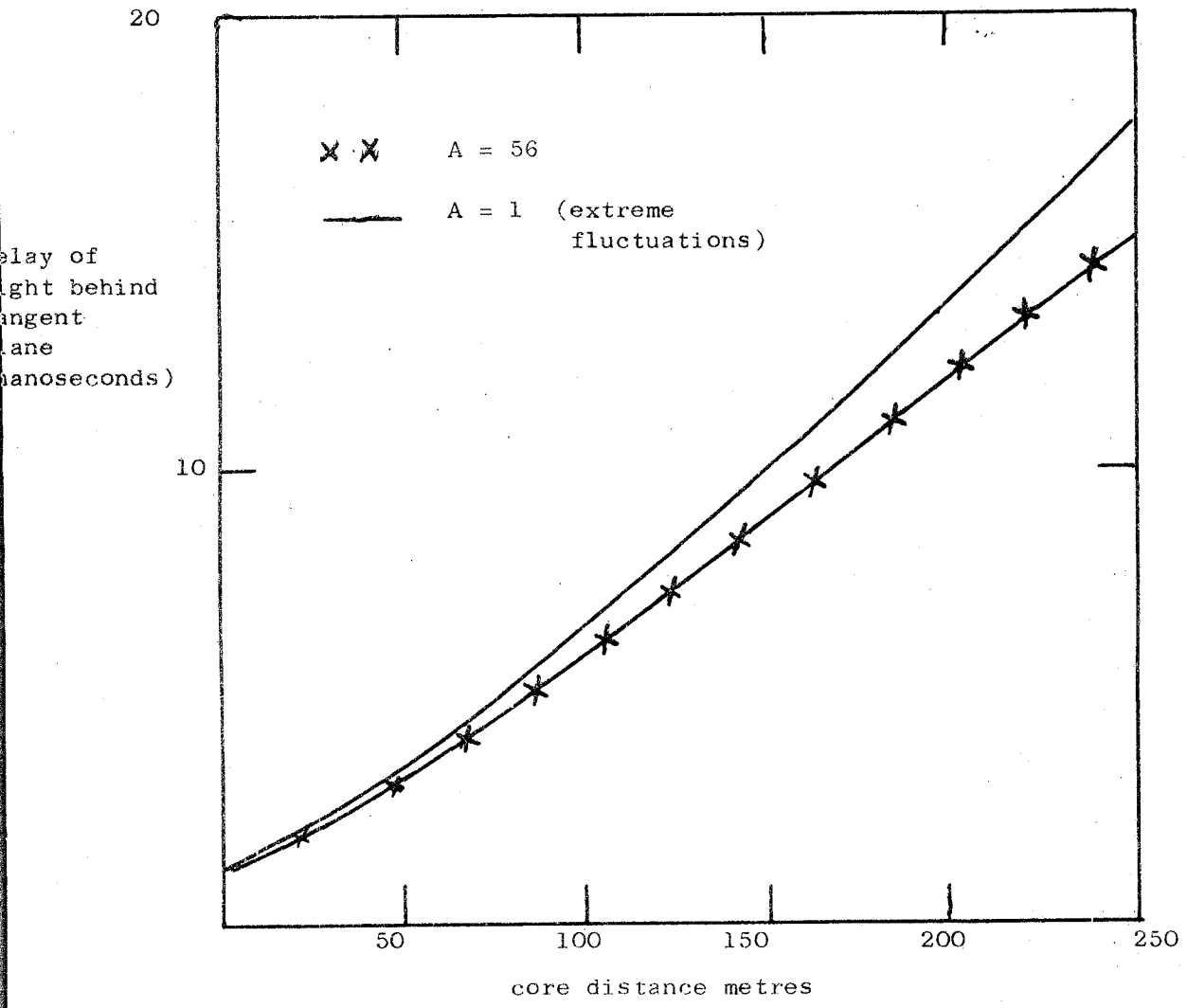
20
10
A = 56
A = 1 (extreme fluctuations)
elay of
ight behind
angent
lane
anoseconds)
50
100
150
200
250
core distance metres

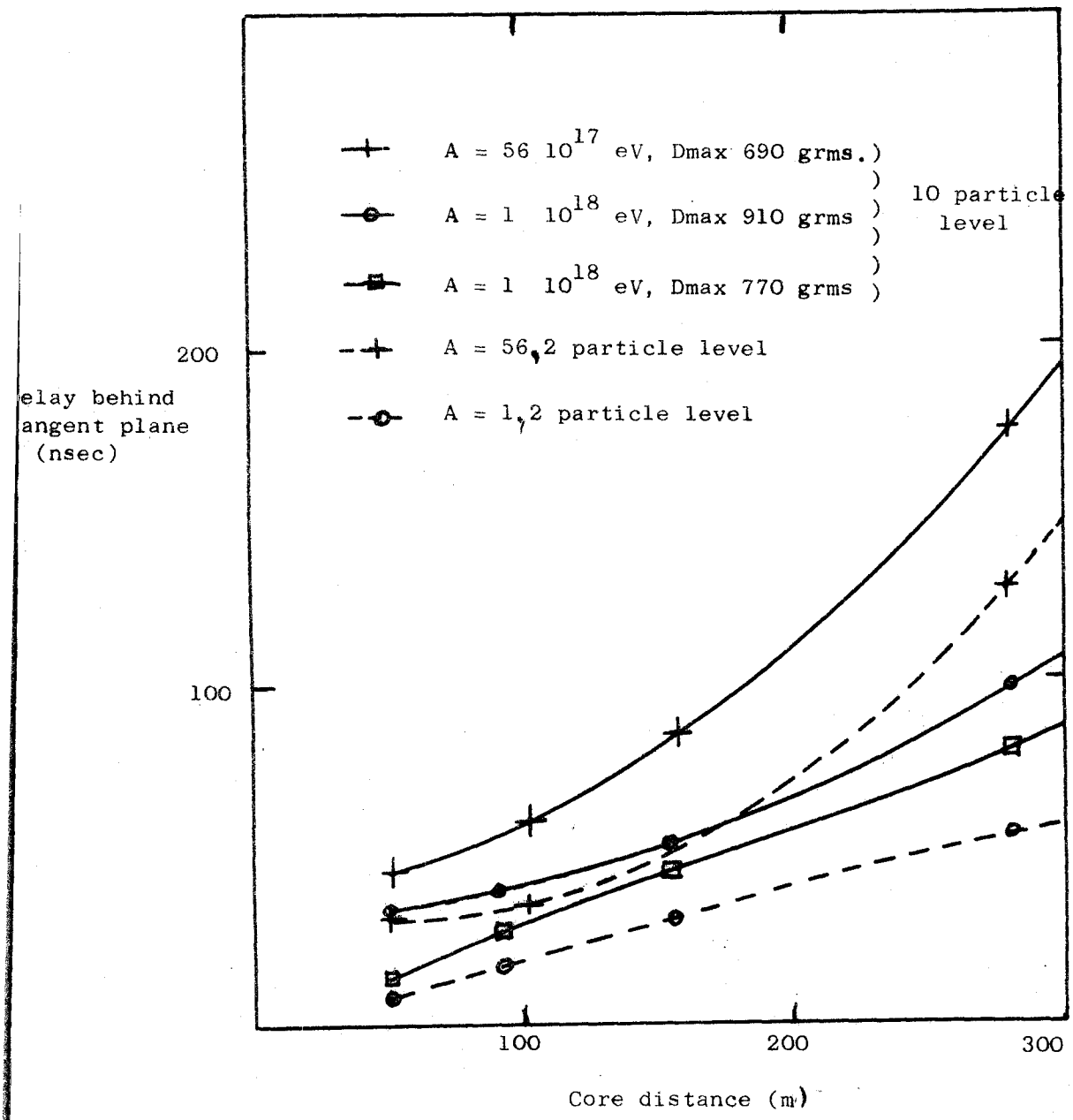
A = 56 10^17 eV, Dmax 690 grms.
A = 1 10^18 eV, Dmax 910 grms
A = 1 10^18 eV, Dmax 770 grms
10 particle level
A = 56, 2 particle level
A = 1, 2 particle level
200
100
elay behind
angent plane
(nsec)
100
200
300
Core distance (m)

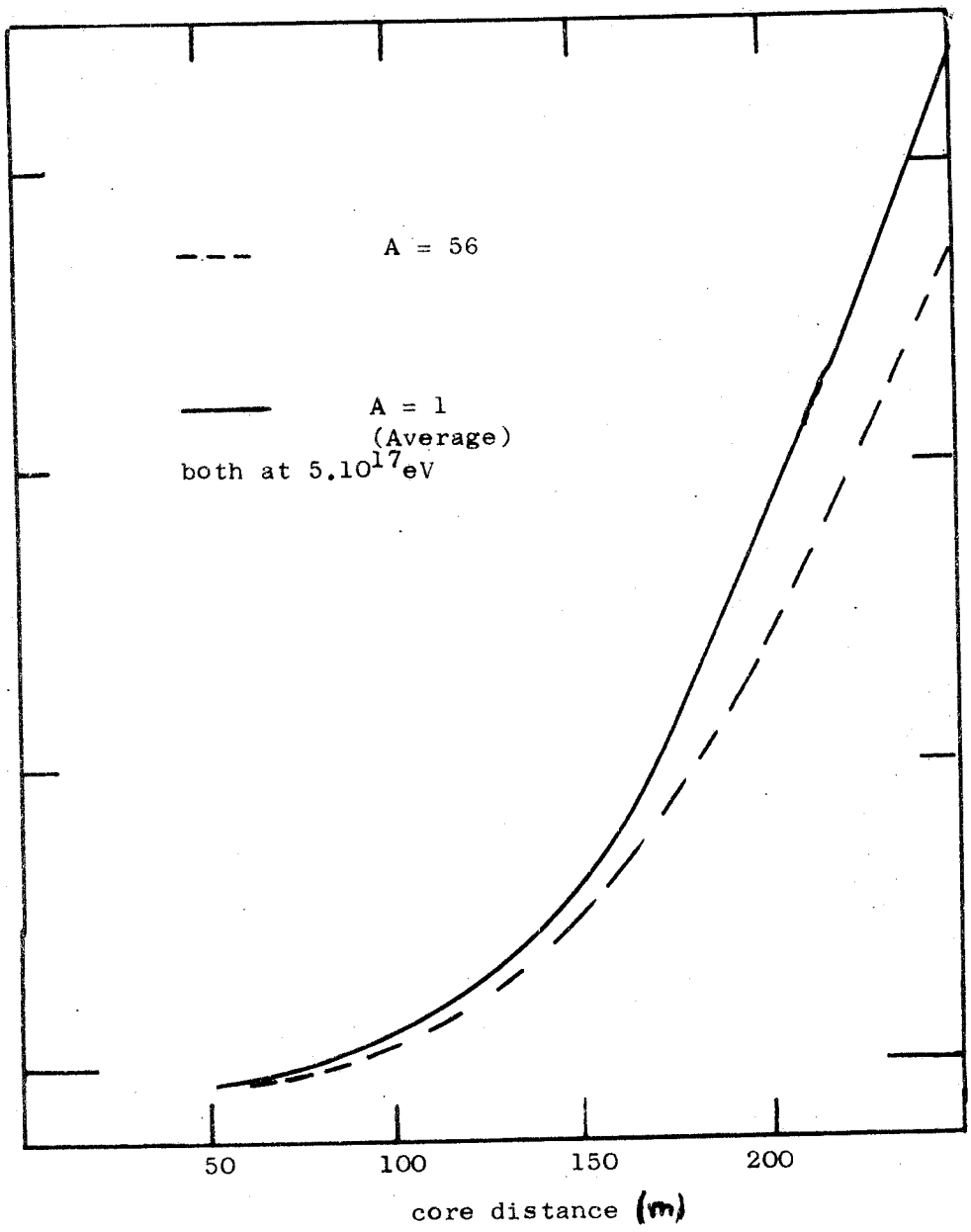

ration
article
light
t.
sec)
tive value
cate light
edes
icles

Figure 3-6 shows the time to the 10% level in the optical pulse for showers of various masses and energies. From this it can be established that this time is virtually invariant with cascade development. So any consideration of change in mass and energy on the time delay can be understood in terms of a change in the development of the electron component. Figures 3-7 and 3-9 show the integral pulse for the electron component for showers of differing masses and energies. From this expected variations in the time delay can be seen. If the arrival time of the particles is said to be when 0.3 vertically equivalent muons (VEM) are incident on 1 m^2 (this is equivalent to the 10 p level in central detectors at Haverah Park), then the following conclusions can be drawn. Firstly, an increase in primary energy will cause a decrease in the delay and secondly an increase in the mass will cause an increase in the delay. These variations are consistent with the brief analysis described above when the changes in depth accompanying a change in either energy or mass are considered.

A more interesting result can be drawn if the time to a particular energy deposition is plotted against depth of maximum. Figure 3-10 shows the situation at 158 m for those showers displayed in figures 3-7 to 3-9, the difference being that the discrimination level in this instance is 0.2 VEM. This indicates that if the delay and the depth of maximum are known, then the mass and energy can be uniquely determined. However, the dashed line indicates the situation for a CKP simulation rather than a scaling model. So although, the situation could be used to describe the mass it is extremely model dependent; but if, for example, a delay of 70nsec with a depth of maximum of 800 g cm^{-2} is observed then although not indicating mass (unless the scaling model was proved) it would rule out the CKP model. It should be said at this point that the broadness of the

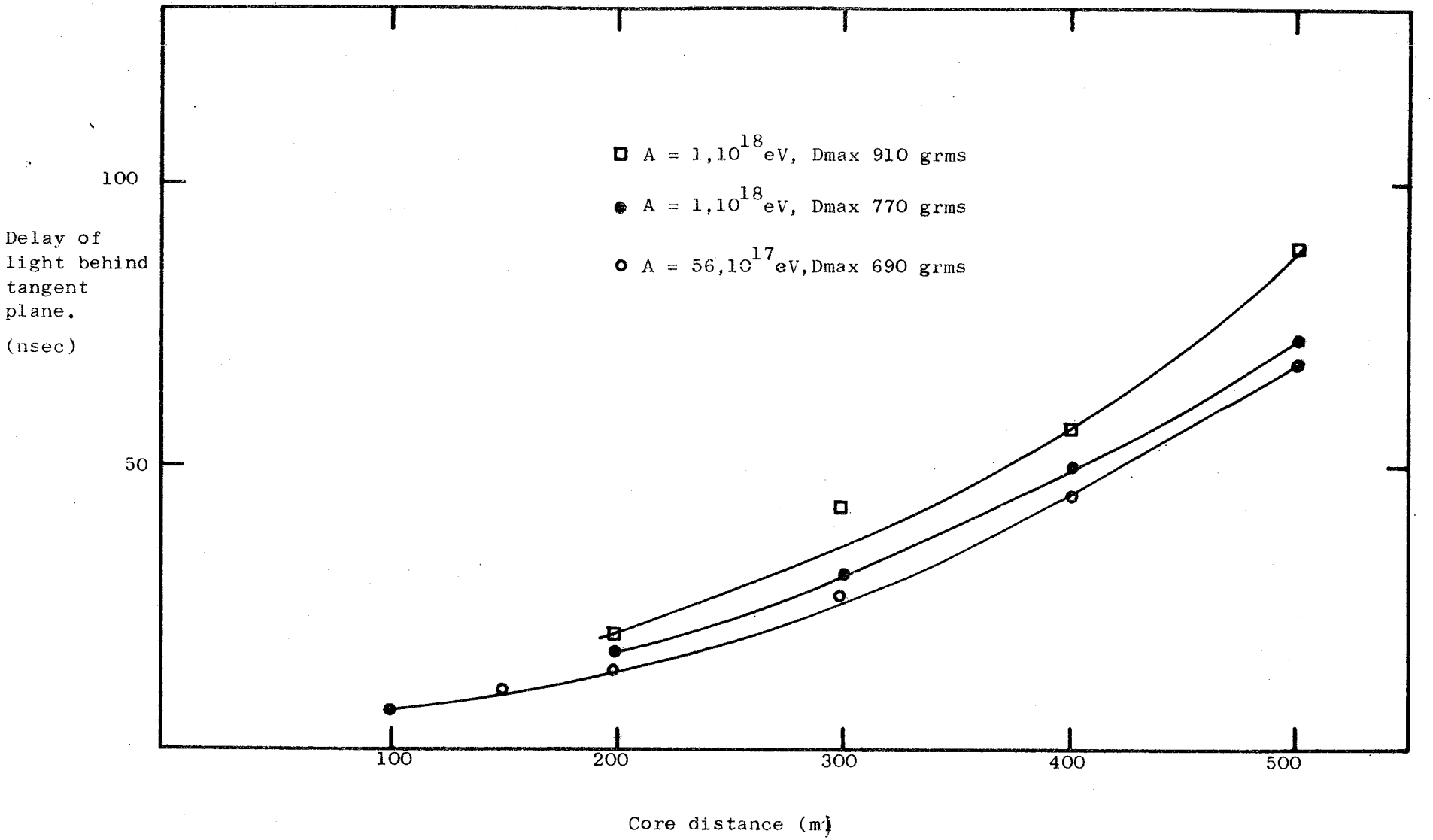
□ A = 1,10^18 eV, Dmax 910 grms
● A = 1,10^18 eV, Dmax 770 grms
○ A = 56,10^17 eV, Dmax 690 grms
100
50
Delay of light behind tangent plane. (nsec)
100
200
300
400
500
Core distance (m)

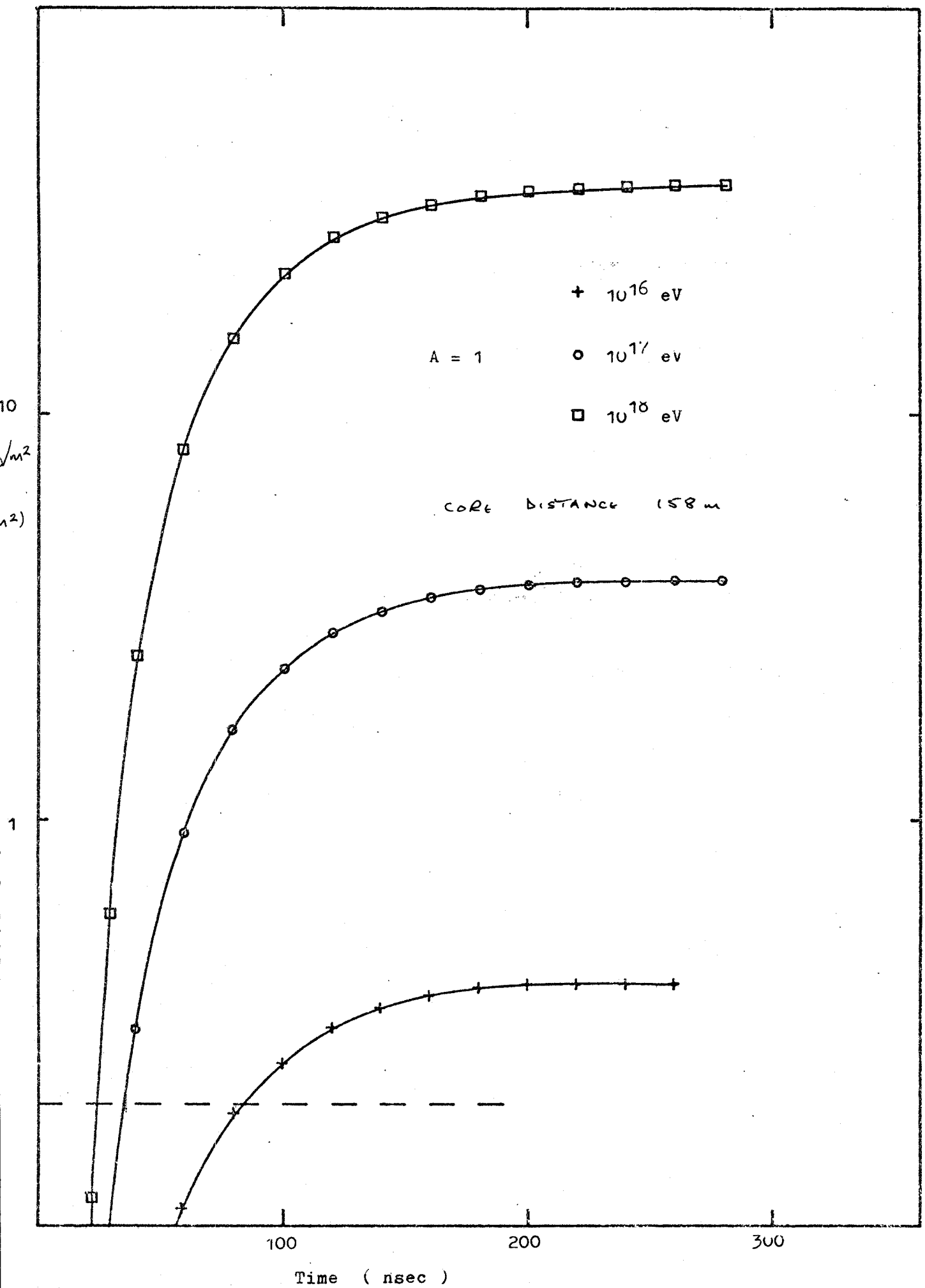
+ 10^{16} eV
A = 1
o 10^{17} eV
□ 10^{18} eV
CORE DISTANCE 158 m
10
1
100
200
300
Time (nsec)

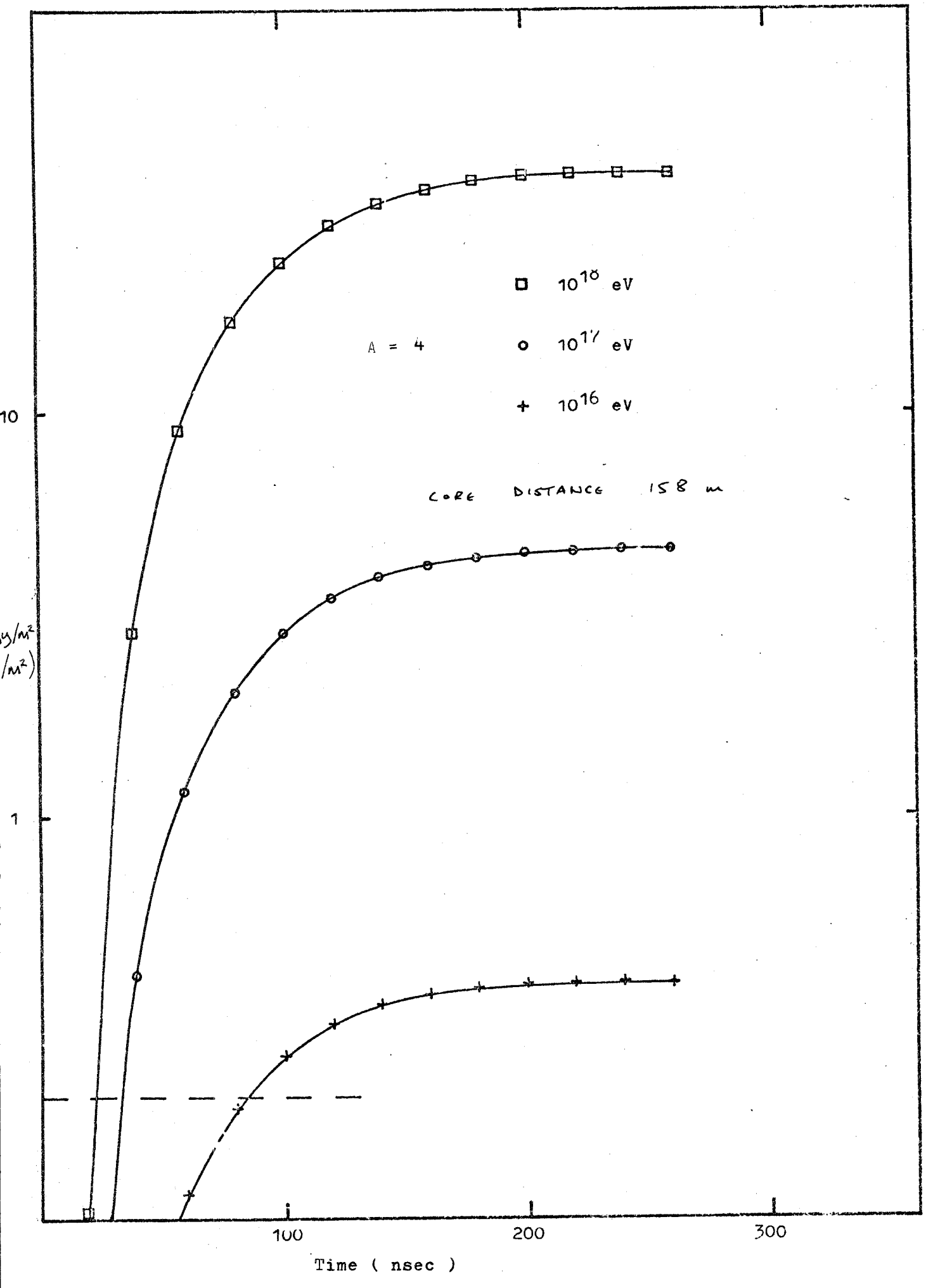
□ 10^{18} eV
A = 4
o 10^{17} eV
+ 10^{16} eV
CORE DISTANCE 158 m
10
1
100
200
300
Time (nsec)

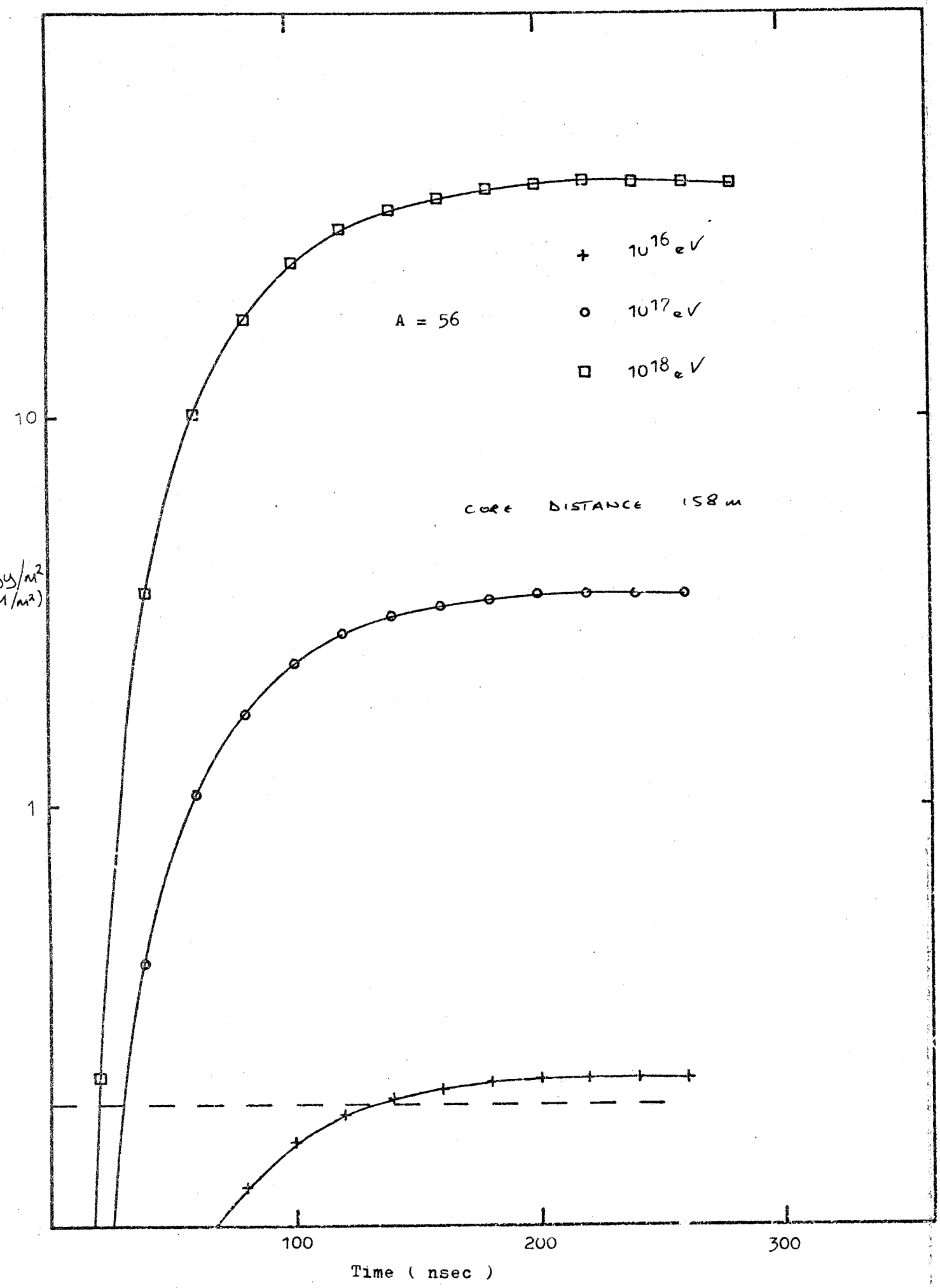
A = 56
+ 10^{16} eV
o 10^{17} eV
□ 10^{18} eV
CORE DISTANCE 158 m
10
1
100
200
300
Time (nsec)

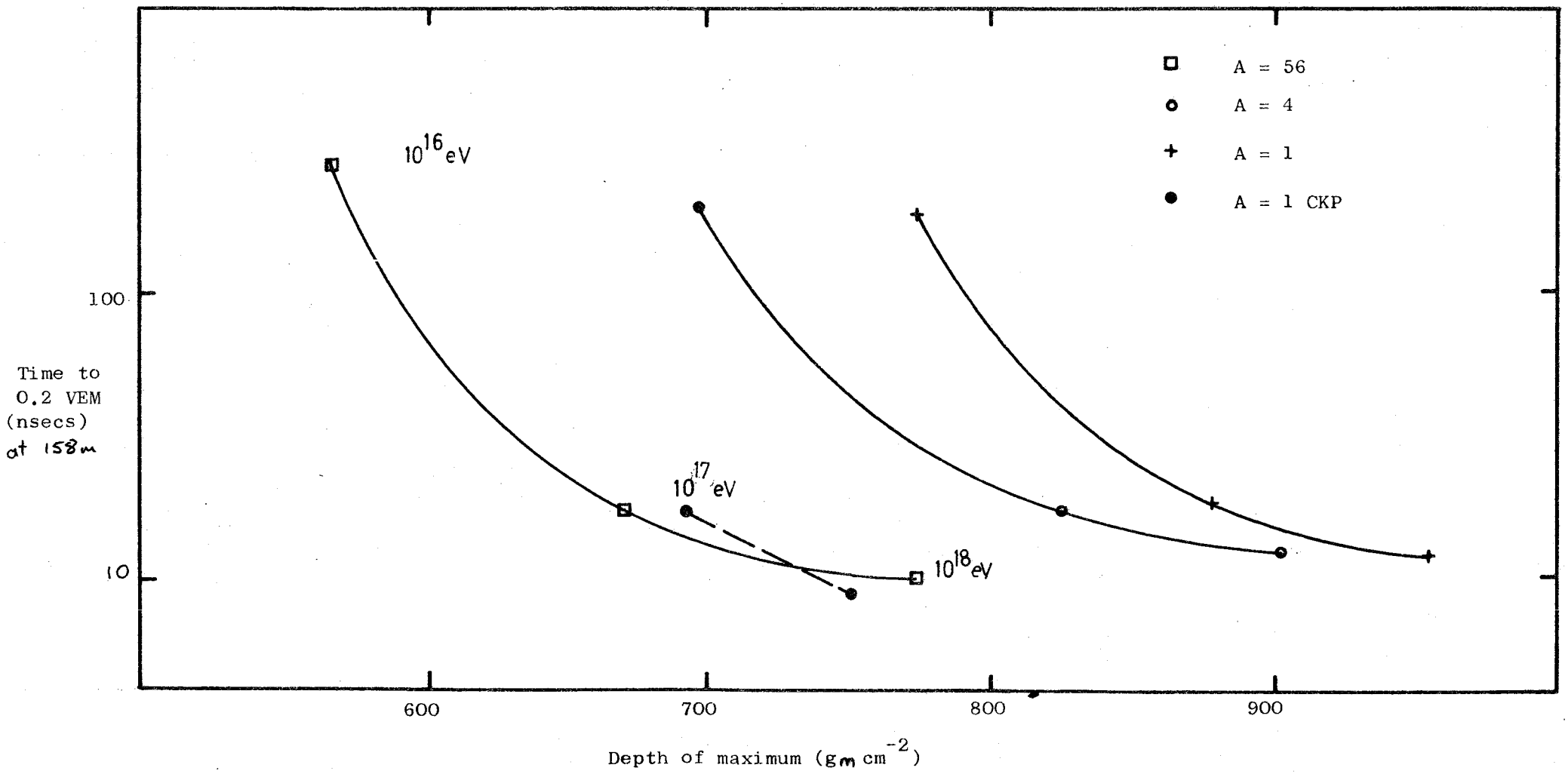
A = 56
A = 4
A = 1
A = 1 CKP
10^{16}eV
10^{17}eV
10^{18}eV
100
10
Time to 0.2 VEM (nsecs) at 158m
600
700
800
900
Depth of maximum (gm cm^{-2})

of the electron pulses shown in figures 3-7 to 3-9 is due to the large collection area used in the simulation. Although this does not effect the leading edge of the pulse, it means that the width of the pulse cannot be determined; a more comprehensive description of the simulation is given in Protheroe (1978).

3.3 Observations of the separation of the light and particle fronts during the winter 1975/76.

During the winter of 1975/76 an array of 8 photomultipliers was operated in conjunction with the particle array at Haverah Park. Figure 2.9 shows the layout of the array during this season. It is beyond the scope of this thesis to describe the array in detail; a description can be found in Wellby (1978), and some of the results were described in section 2.3. Although no separate experiment was devised to measure the delay between the two fronts it was possible to measure the separation by considering the triggering arrangements of the optical detector array. This arrangement is shown in figure 3-11. The triggering of the recording oscilloscopes occurred a fixed time after the 10 p level was achieved in the central 34 m^2 of deep tank detector. Although there was then no detector situated in the vicinity of the central particle detector, there was one situated at hut 12 (see figure 2-9) 50 metres distant from the centre of the array. By assuming a plane front for the light over this short distance, it was possible to transform any timing information from hut 12 to that expected if the detector had been situated at the array centre. Thus the time of the start of the sweep of the recording oscilloscopes can be related directly to the 10 p level, so the distance along the time-base of the oscilloscopes from the sweep start to the 10% level in the hut 12 optical pulse can be related to the delay between the particle and light fronts. The optical pulse is delayed by an amount slightly greater than the coincidence window, this was to enable the optical pulse to be positioned well into the

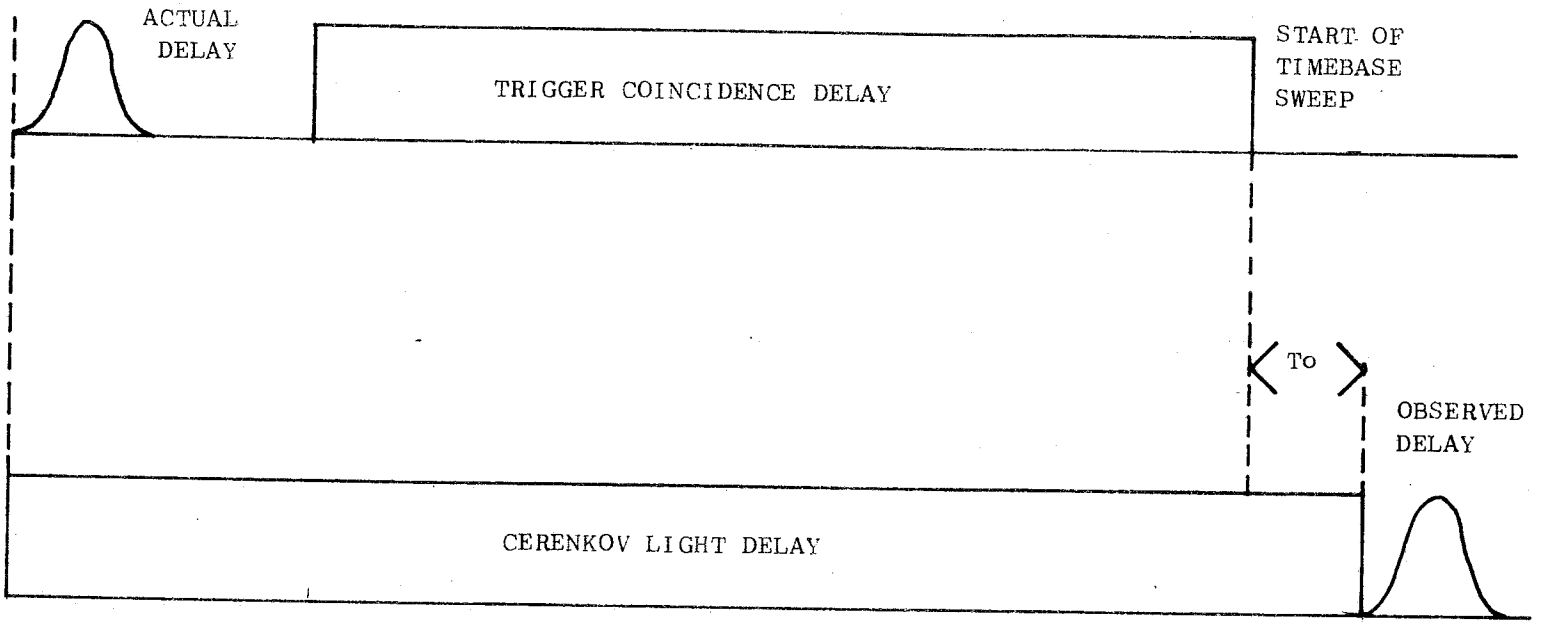
ACTUAL
DELAY
TRIGGER COINCIDENCE DELAY
START OF
TIMEBASE
SWEEP
To
OBSERVED
DELAY
CERENKOV LIGHT DELAY

sweep of the oscilloscope. So, if the particles and light were coincident at ground level then the optical pulse would be at a time T_0 along the time-base, where T_0 is the length of the coincidence window minus the total delay of the optical pulse. From this the actual delay between the two fronts is given by:-

$$\text{Time Delay} = T_0 - T_{obs}$$

3.3.2 Selection criteria for observed events

In this study, as nanosecond accuracy was desirable to obtain an accurate determination of the nature of the delay, it was thought essential to use only those events which satisfied rigid selection criteria. The criteria used were established to ensure that the events chosen were consistently accurate in all parameters. Firstly, because of the response time of the deep water tanks a large particle density in the central detector was considered to be important. In view of this no events were used which had a central density less than ten times the threshold level (10p).

The accuracy of core location would also effect any conclusions as the delay has a strong core distance dependence. So events were rejected if they fell outside the confines of the 500 metre particle array. Events with a large zenith angle ($\theta > 40^\circ$) were also rejected.

3.3.3 Results 1975/76

During this winter a total of 17 events were recorded, which, satisfied all the selection criteria described above. Figure 3-12 shows the observed delay, normalised for the reversal described in section 3.3.1, plotted against core distance.

A multiple regression of the observed delay against r, p(500) and θ gives:

$$t_d(r, \rho(500), \theta) = 12.2\ r^{.345}\ \rho(500)^{-.136}\ \sec\theta^{.526} - 100\text{ns} \quad \text{Equ. 3.1}$$

Standard error on estimate 1.5 nsecs, s.d. 6 nsecs.

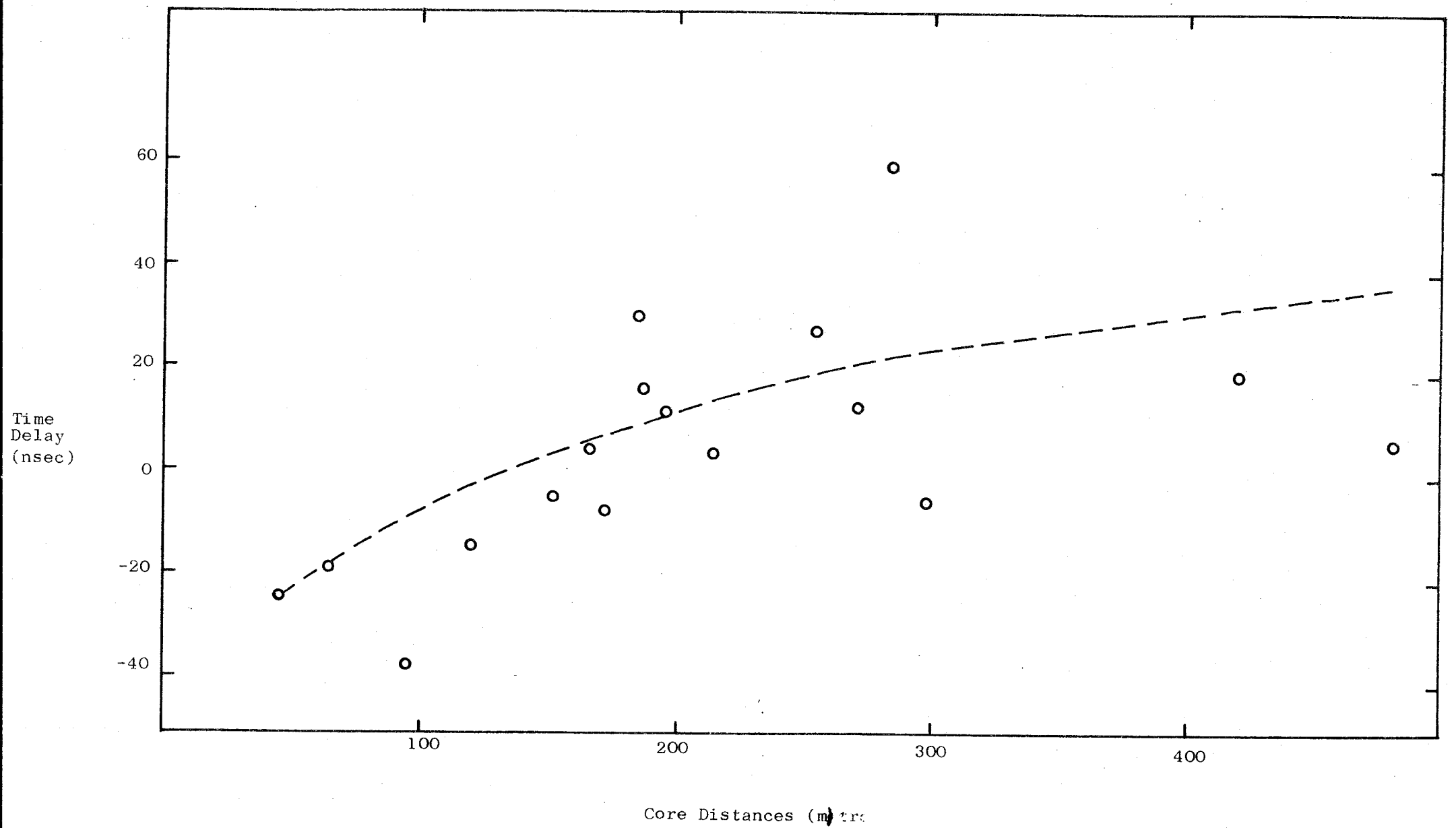
60
40
20
0
-20
-40
Time
Delay
(nsec)
100
200
300
400
Core Distances (m)

3.4. Individual shower measurements

The technique described above only allowed for a single measurement to be made within one shower, thus only the average characteristics of a sample of showers can be estimated. However, for a small sample of showers further measurements could be made within showers. The individual particle times for detectors 2,3 and 4 were recorded for the zenith angle and azimuth determination of the University of Leeds particle array.

These particle detectors were colocated with atmospheric Cerenkov detectors; consequently, when there exists a coincidence between a particle and light response it was possible to measure the front separation across the shower. The problems of timing inaccuracies resulting from low particle densities are increased for these detectors as they tend to be further from the core of a shower and consequently have low recorded densities. The times used in this section do however correspond to the 2 p level so that a lower density criteria can be used. Due to the sparcity of events of this sort, the criteria described in section 3.3.2 were relaxed so that events were only rejected if the local density was less than 5 times the threshold. Consequently all the results described in this section should be regarded as exploratory. As it was impossible to calculate with any degree of certainty the absolute value of the delay at each location it was decided to study the gradient of the parameter with core distance. This was achieved by normalising the particle and light times so that at the array centre both the particle and light times were identical to zero. After this the two fronts were subtracted at each location, thus giving a measure of the delay at various points on the ground. Figure 3-13 shows the relationship between the delay and core distance for 8 showers; the delay here is $T_{light} - T_{particles}$

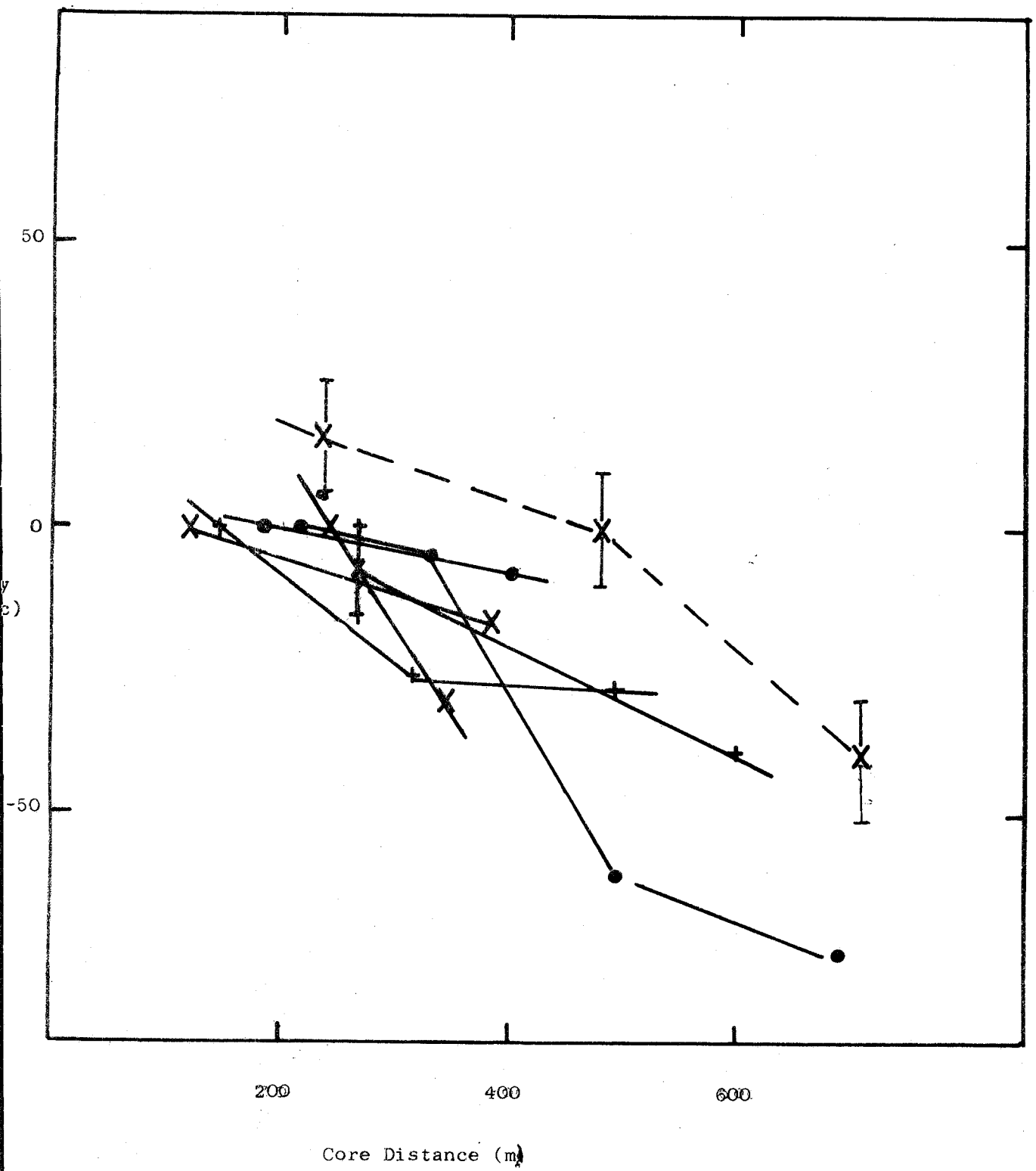
50
0
-50
200
400
600
Core Distance (m)

as the delay has been normalised, a negative value does not necessarily imply that the particles arrived before the light. The average slope was found to be 19.6 nsec increase in this delay per 100 metres change in core distance.

- CHAPTER FOUR -

Further measurements of the separation of the light and particle fronts

Following the exploratory work described in the previous chapter it was thought that more accurate results would be obtained using a detector with more accurate timing capabilities - a plastic scintillator. This chapter describes the first attempts at making such measurements during the winter of 1976/77 at Haverah Park. A comparison with other parameters is given as well as a discussion of the results from the two seasons.

4.1 Scintillators versus Deep Water Detectors

Before describing the results of this experiment it is necessary to consider the relative merits in this context of a plastic scintillator when compared to the deep water detectors at Haverah Park. The main advantage of a scintillator is its fast response to a particle flux, which, in the context of this experiment was extremely important. A scintillators bandwidth is effectively limited by the bandwidth of the photo-multiplier which detects the scintillation light, in this instance a type 53 AVP having a rise time of less than 2 nanoseconds. The scintillator will also respond to the passage of one electron, although this facet was not heavily relied upon. The deep tanks at Haverah Park detect the Cerenkov light emitted by a charged particle as it traverses 1 metre of clear water. To detect the light photomultipliers are dipped onto the surface of the water, the photomultiplier will then detect the light after it has been reflected off the sides. If has been estimated that the light will undergo seven reflections before it is incident on the face of the photomultiplier, Tennant (1968). It is this straggling of the light paths which accounts for the slow response time of the tanks. It was this slow build up of a pulse which prompted the change to a plastic scintillator for timing the arrival of the particles.

However, the deep tanks have a strong advantage, in that their relatively cheap cost of production facilitates the use of large detecting areas, 34 m^2 in the case of the 500 metre array at Haverah Park. The scintillator used in this experiment had an effective area of 1/3 m^2. It is to be expected that the timing accuracy will, to a large extent, depend on the local electron density around a detector. If the local electron number is less than, say, 10/m^2 then, it is reasonable to assume that any of the detected electrons would have come from any part of the shower disc; if a disc of 3 metres thickness is considered, Bassi et al (1953), then this could lead to a timing jitter of 20 nanoseconds. If conversely, the density was in excess of 50/m^2, then it would be expected that at least some of the detected electrons would have come from the leading edge of the disc. Figure 4-1 shows the expected electron number plotted against core distance. From this, we see that if a core distance of 250 metres is used as a maximum, then there will always be in excess of 20 particles in the detector. The geometrical projection of the detector in an inclined shower has also to be considered. If a shower is incident on the array at an angle of θ then the effective area of a thin detector reduces by a factor of cos (θ). If a maximum local zenith angle of 30 degrees is considered then the core distance criteria mentioned above would reduce to about 220 metres.

4.2 Initial Observations 1976/77

During the winter of 1976/77 a few minor modifications were made to the atmospheric Cernekov light array. The major improvement being the relocation of the central photomultiplier from location 12 to location 1 in figure 2-9, the centre of the particle array. To improve the dynamic range of the outer detectors, 7" photomultipliers in conjunction with 1/2 metre dishes were situated alongside the existing 5" photomultipliers. A full description of these improvements will be found in Waddoup (1978).

In October 1976 a plastic scintillator, of area 1/3 m^2 was operated

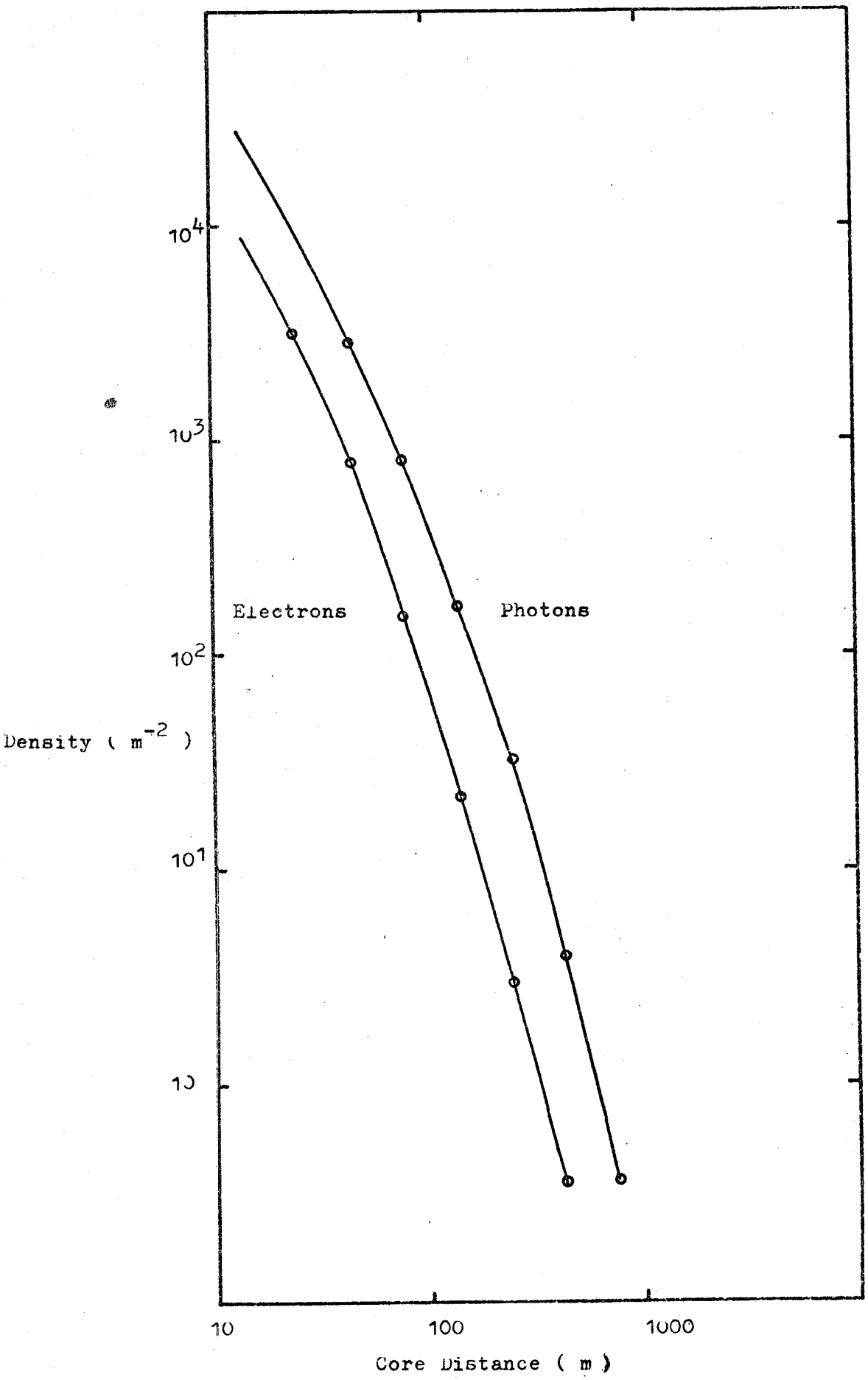
10^4
10^3
10^2
10^1
10
Electrons
Photons
Density (m^{-2})
10
100
1000
Core Distance (m)

in the vicinity of a 7" photomultiplier viewing the night sky directly. The purpose of this activity being to investigate the feasibility of using such a small particle detector for timing measurements, the apparatus was run separately from the main Cerenkov array so as to cause a minimum of disturbance. The outputs of the two detectors were separated by delaying the scintillator response by approximately 100 nsecs. After this delay the two signals were mixed and delayed for about 2 μseconds using a lumped delay line, the final signal being displayed on a fast recording oscilloscope and photographed. The extra delay was used so as to enable the 150 metre particle array to make a coincidence. The low bandwidth of a delay line does not effect the short timing measurements being made, as relative arrival times are being considered rather than detailed pulse structures. During the period of running of this arrangement of detectors no shower data were available as the triggering came from the 150 rather than 500 metre array and shower analyses are only available for 500 metre events. This means that no comparison could be made with conventional shower parameters. However, by considering the coincidence criteria and the geometry of the 150 metre array, an expected median core distance of the detectors can be estimated for a distribution of showers. The two detectors were situated at location 12 in figure 2.9. A triggering of the optical array occurred when there was a coincidence between the centre and any two of the three 150 metre particle detectors. If it is assumed that on average a shower will cause a three-fold coincidence if it falls within 150 metres of the three tanks, then most of the showers recorded will lie between 100 and 300 metres of location 12, the peak of the distribution would be about 200 metres.

To obtain the exact delays of the two detectors, it was necessary to measure the propagation times of the two detectors. This was achieved by flashing a light emitting diode in the field of view of the atmospheric

Cerenkov photomultiplier and in the scintillation material. From this the relative propagation times were obtained; consequently the actual separation of the particle and light front could be seen. Figure 4-2 shows the observed distribution of times, normalised for propagation delays.

4.3 Observations of the time delay in conjunction with the main Cerenkov light array

4.3.1 Introduction

In order to understand more fully the relationship between the separation of the two fronts and shower parameters, it was necessary to operate a scintillator in the vicinity of a night sky photomultiplier whilst the main particle and Cerenkov array were running. It was thought important to have both particle and night sky Cerenkov detector information to enable correlations to be made with conventional shower parameters and the new information related to the longitudinal development of a shower coming from studies of the temporal structure of the Cerenkov light pulse. To minimise the data analysis it was thought prudent to locate the scintillator with one of the main Cerenkov light photomultipliers; from core distance considerations it was decided to locate the scintillator at the centre of the array, near to the central photomultiplier and the central deep water tanks. To ensure a minimal disturbance of the optical array, it was decided to display the arrival time of the electrons as a time marker triggered by the scintillator. This marker, a 10 nanosecond wide pulse, was delayed by about 100 nanoseconds to avoid any interference with the optical pulse. The time marker and the optical pulse were then mixed in situ after the latter had been amplified. The combined outputs were then sent down approximately 50 metres of high quality cable to the recording station. Here the pulses were delayed using high quality cable, for about 2 microseconds to position the pulses within the display window generated by the 150 metre particle array.

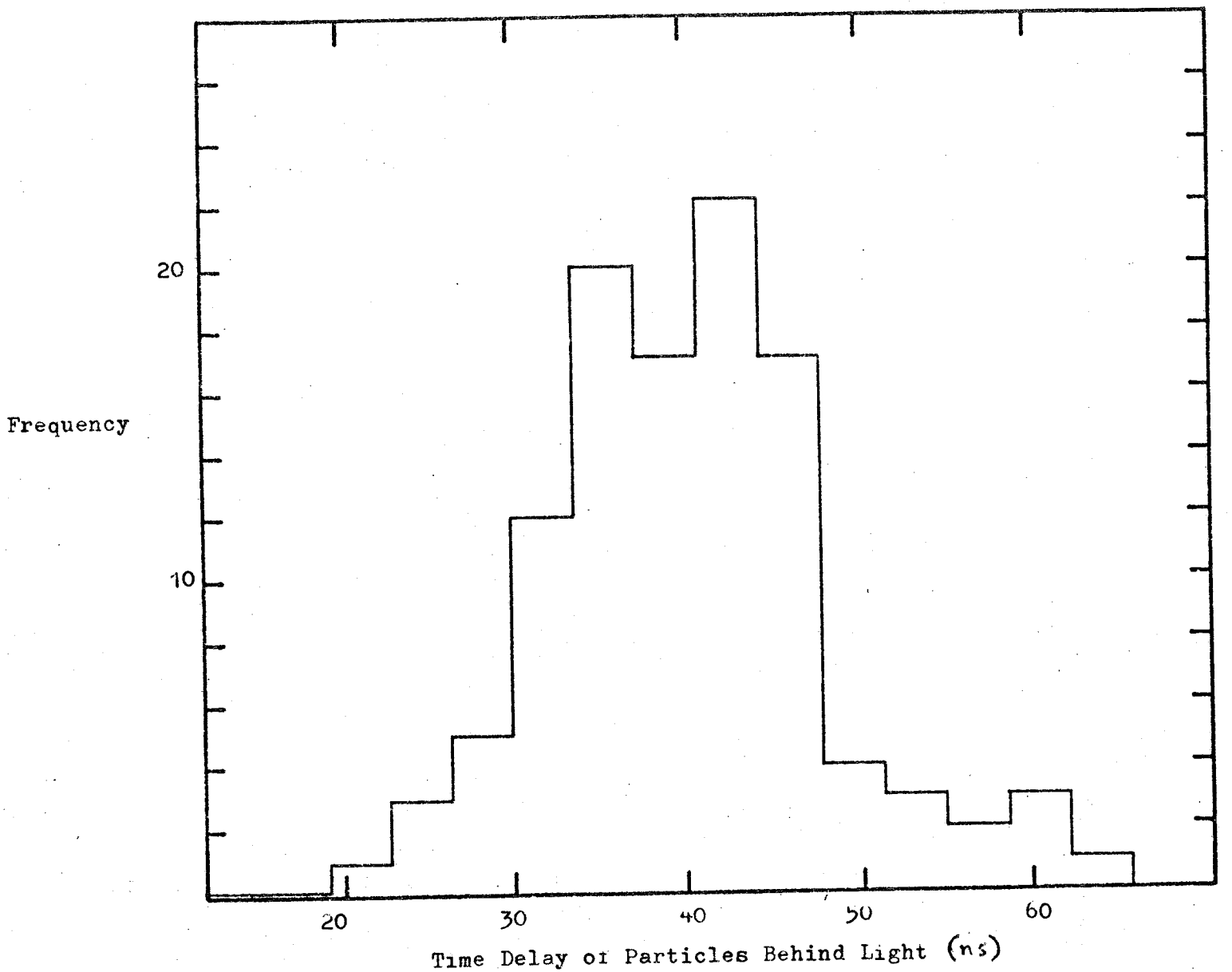
Frequency
20
10
20
30
40
50
60
Time Delay of Particles Behind Light (ns)

To analyse the traces, the photographs of the oscilloscope screen were enlarged to about twice life-size and measured using a standard graticule. The oscilloscope time base velocity was 100 nanoseconds /cm. and approximately 60 nanoseconds / cm after enlargement. The exact print timebase could be measured using accurate timemarkers displayed on each trace. Prints could be measured to better than 0.5 mm, thus allowing for timing accuracies better than 5 nanoseconds.

4.3.2. Results - Early 1977

The Cerenkov array was running for about 60 clear moonless dark hours, and for about 20 of these the scintillator was integrated into the system. During this winter 19 showers occurred which had sufficient Cerenkov data for a full analysis of the type described in section 2.4, and 9 of these had a coincident particle marker. In addition to these a further 2 events were in coincidence with a main array event with particle analyses from the Leeds University group. Five of the 9 Cerenkov events also had particle data available.

As the time delay was a new parameter it was thought wise to make initial comparisons with shower analysis based upon particle data rather than the Cerenkov light data. (This also allowed a more direct comparison with the results of the previous year.) During this phase of the experiment no attempt was made to measure absolutely the propagation delays through the photomultiplier and the scintillator. This does not affect the results to be presented as only qualitative conclusions were sought and only the gradients of any relationship will be considered. Figure 4-3. shows the relationship between the observed time delay as seen with the scintillator and the time delay deduced from the position of the optical pulse along the timebase. This latter measurement is identical to the measurements presented in the last chapter, except that the abissca has not been normalised for timebase reversal. As both abissca and the ordinate represent measurements of the same thing, then it would be expected that

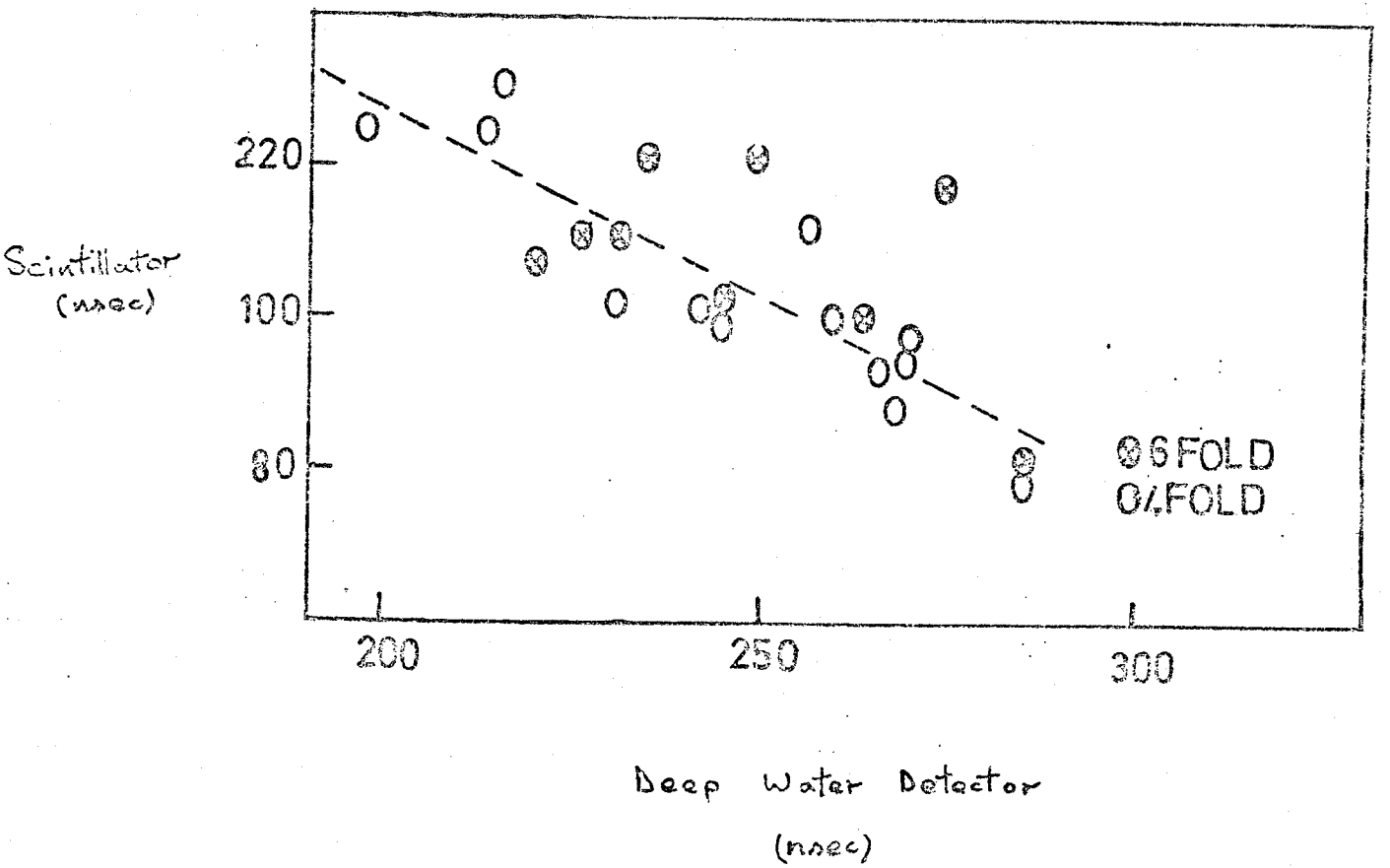
Scintillator
(nsec)
220
100
80
200
250
300
Deep Water Detector
(nsec)
6 FOLD
4 FOLD

the gradient of the relationship would be unity. The slope, as the time to the optical pulse is reversed, should be, as observed, negative. The situation in comparing the separation as measured by a scintillator and the deep tanks is similar in concept to comparing the time to the 10 particle and 2 particle levels in the deep tanks. Figure 3-4 showed the time to these values for 10^{18}eV proton shower. From this it is clear that for increasing core distance with a similar type of detector the time difference between the 2 and 10 particle levels increases. This time will be further increased if the detector for the 10 particle level has a much slower response time, as is the case. These two effects will move the observed delays in figure 4-3 to the right thus reducing the value of the slope.

Figure 4-4 shows the relationship between core distance and the separation for events having a 500 metre array response. The multiple regression of the time delay upon shower parameters was found to be:-

$$TD = 3.4\ r^{0.248}\ \rho(500)_{ve}^{-0.076}\ (\sec\theta)^{-1\cdot12} \quad \text{nSec.}$$

(standard error on estimate 1.2 nsec , standard deviation 4 nsec)

The small number of observed events coincident with Cerenkov showers prevented any accurate comparison with the data related to the longitudinal cascade.

4.4 Conclusions from 1975/76 and 1976/77

4.4.1 Introduction

The results presented in the previous chapters indicate that the time delay between the particle and atmospheric light fronts is a readily measurable quanity. Although a particle detector with poor timing capabilities was used initially, convincing correlations were made with conventional shower parameters. The results obtained during the winter 1976/77 indicated that a small area particle detector could be also used to measure the delays at small core distances.

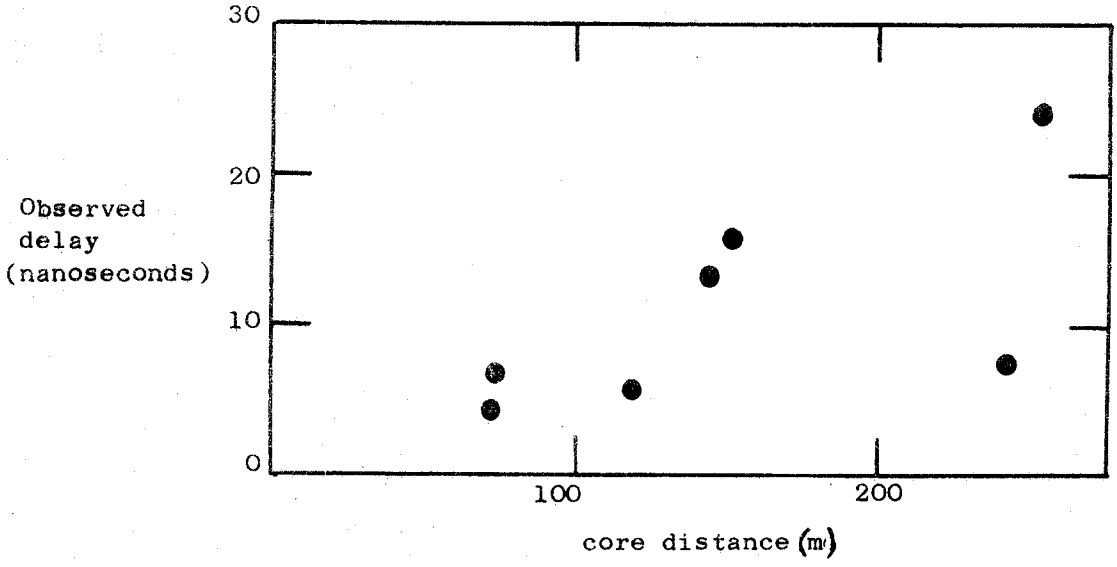
30
20
10
0
Observed
delay
(nanoseconds)
100
200
core distance (m)

4.4.2 Analysis of 1975/76 Data

The relationship between core distance and time delay shown in figure 3.12 can be understood in terms of the superimposition of two fronts of differing curvature. Figures 3-2 and 3-3. showed the calculated delay behind the tangent plane for particles and Cerenkov light. By differing these it was possible to obtain the calculated delay between the two fronts. At shower energies of 5×10^{17} eV, for core distance of 100-200m this was found to lie between 25 and 30 nanoseconds for protons and about 25 nanoseconds for iron. The observed delay at this energy ($\rho(500) = 1 \ m^{-2}$) was found to be 23 nanosecond atdistances between 100 and 200 metres, in close agreement with simulation results.

Any change of a parameter with $\rho(500)$ and zenith angle relates to the different developments of the shower through the atmosphere.

The time delay was observed to decrease by 27 nanoseconds for an increase of one decade of primary energy, at 158 metres core distance. Figure 3-7, showing the effect of an increase in energy from 10^{17} to 10^{18} eV, indicates that within this energy range the delay should decrease by about 20 nanoseconds over the decade at a core distance of 158 metres. When it is considered that the range of observed energies in this sample was from 5×10^{16} to 5×10^{17} eV in this case the expected decrease should be greater than that for 10^{17} eV to 10^{18} eV. This shows that the observed delays are in close agreement with the results of simulations.

A relationship between the observed delays and zenith angle was also noted. A change in zenith angle will cause a change in the thickness of the atmosphere through which the shower develops beyond mazimum. Zenith angle can be related to changes in depth of maximum position above the observation level.

Atmospheric thickness (g cm^{-2}) = 1030. sec (θ)

This change in zenith angle can be directly related to a change in terms of gm cm^{-2}. The observed relationship between time delay and zenith angle can therefore be related to a variation with cascade development. At about 10^{17} eV and at a core distance of 200 metres the time delay increases by about 5 nanoseconds for 100 grammes of extra atmosphere between depth of maximum and observation level. All these results are summarised in Table 4-1.

The measurements of the delay at different points within an individual shower were discussed in section 3-4. Although the results presented were of a very preliminary nature certain indications should be noted. The mean gradient was found to be 19 nanoseconds/100 metres, in close agreement with the values from simulations described above. There was no possibility of observing a change in the gradient with primary energy as all the delays were normalised so that any offset due to a primary energy would be lost.

4.4.3 Analysis of 1976/77 data

The first conclusion from the observations made during this season is that, from figure 4-2 a mean value of the delay in showers of about 3.10^{17} eV, was 40 nanoseconds with a standard deviation of 18 nanoseconds. The expected core distance for this sample of showers was within the region 100-300 metres. Figure 3-5 showed the calculated delay for a $5x10^{17}$ eV proton initiated shower of 40 nanoseconds at 200 metres.

The 8 showers with a measurement of the delay as well as a particle analysis from the University of Leeds group were correlated in the same manner as the events described in the previous section. The actual coefficients of the correlation are however significantly different. This can be understood as the quantity being measured is different in the two

seasons. During 1975/76 the delay was measured from the 10 particle level in the deep detectors and during the season 1976/77 from a discrimination level set just above the noise from the output of the scintillator; this was lower than the 10 particle level in terms of energy deposited for discrimination. The situation is similar in concept to comparing the delay measured from the 10 p and the 2 p levels. Figure 3-4 showed the effect on the separation of lowering the discrimination level from 10 p to 2 p. From this it can be seen that the gradient of the relationship front separation versus core distance is reduced if the discrimination level is lowered. Also by considering figure 3-7 showing the time to a particular energy deposition at 158 metres, it can be seen that the exponent of the front separation versus energy ($\rho(500)$) function should decrease with decreasing threshold.

The function shown in section 4.3.2. for TD ($r, \rho(500), \theta$) has an increased exponent for the r and $\rho(500)$ terms. The apparent change in sign of the zenith angle term exponent has not been explained. Further work will have to be done to confirm this change, although as the expressed effect of zenith angle is small and it is conceivable that the smallness of the data set could mask any of zenith angle effects.

Table 4-2 summarises the information presented in the previous two sections. No attempt has so far been made to measure the errors occurring in this study. It has been estimated that print measuring accuracies are of the order of 4-5 nanoseconds after adjustment for timebase non-linearity has been made. So the standard error of 1.2 nanoseconds and the standard deviation of 5 nanoseconds is of the same order as the expected print measuring inaccuracies. It would require a much larger sample of obtain a quantative estimate of the experimental

errors. However, even from this limited sample of showers it can be seen that the separation of the two fronts is an observable quantity, which varies according to the expectations of simulations and simple arguments concerning basic shower development.

TABLE 4-1

Comparison of simulation with experimental determination of the time delay.

A	nsec/100m @ 10^{17} eV	nsec/decade in energy 10^{17} - 10^{18} eV	nsec/decade 10^{16} - 10^{17} eV	nsec/100gm (from zenith angle)
1	28	20	50	5
56	25	20	50	-
Observed	23	(27	27)	5

TABLE 4-2

Comparison of results from two seasons of observation for fronts to standard shower parameters

	Fit to $T_D = A r^{\alpha} E_p^{\beta} (\theta)^{\gamma}$ ns			
	A	α	β	γ
1975/76	12.2	.393	-0.136	.526
1976/77	3.9	.248	-0.076	-1.12

- CHAPTER FIVE -

Future Work

It is the intention in this chapter to outline the future developments of the studies of Cerenkov light to be carried out by the Durham University group. A description of a new experiment which has been deployed in the U.S.A. is given, as well as a description of how a small array of detectors measuring the separation of the two fronts will be incorporated into this experiment.

5.1 The problems of observing Cerenkov light at Haverah Park

Studies of Cerenkov light, although having the advantage of a flux 10^5 times that of the particle flux, have serious difficulties as the observations have to compete with the general night sky brightness, 10^4 photons m^{-2} s^{-1}, and scattered man made light. That some of the light originates high in the atmosphere means that observations must be made during cloudless conditions. From these two considerations it can be seen that the perfect observational setting would be one far removed from sources of man-made light and in a climate which allows for long periods having clear skies. Neither of these prerequisites are satisifed at Haverah Park, which is situated about 3 miles from Harrogate and has about 10 clear moonless nights through the winter. To put these considerations into perspective during the winter of 1975/76 only 60 hours of reasonable weather and moonless conditions existed. This gives a duty cycle of $\approx$2%. When it is considered that during this period the array had to be kept at full operating specification, it is obvious that this is expensive in terms of manpower and cost.

An experiment has been developed, which, is deployed at a site of good 'seeing' in the U.S.A. It is expected that the array efficiency will be greater than 10%. A further change in the new experiment has been the shift from analogue to digital recording techniques.

5.2 Analogue . vs. digital recording techniques

The present array at Haverah Park relies on a combination of delay cables, oscilloscopes and cameras to record an EAS. This combination reduces severely the bandwidth of the system. The major limitation being the 500 metres of delay cable, although the cables are of exceptionally high quality (Delta Enfield 4303's) the response to a 2 nanosecond wide spike has been found to be a rise time of about 9 nanoseconds and a FWHM of 18 nanoseconds. With the development of studies of the temporal structure of the light pulses, see Orford and Turver (1976), it has become essential that any new system has a superior temporal response. Obviously if the pulses could be analysed locally, at the detector, then there would be no limitation coming from the use of long lengths of cable. It was decided therefore that the new experiment would analyse the pulses in situ and store the information in a digital format.

The major disadvantage of a digital system being that with an analogue system an a posterori decision is required to decide what parameters can be usefully measured, whilst a digital system requires an a priori decision. An analogue recording technique is more flexible as any parameter within the bandwidth of the system can be measured, whilst, with a digital technique any additional experiments have to be integrated into the system, possibly at great cost. This implies that before embarking on designing a digital system careful consideration has to be given as to whether the new system is measuring parameters which can be effectively analysed. In the new experiment the Cerenkov pulse will be reconstructed by measuring the charge within narrow (5-10 nanosecond) sequential slices through the signal from the photomultiplier. Figure 5-1 shows a possible configuration of these slices. As well as these slices the system will measure the total pulse area and time of arrival. Consequently, a conventional analysis can be carried out using the area

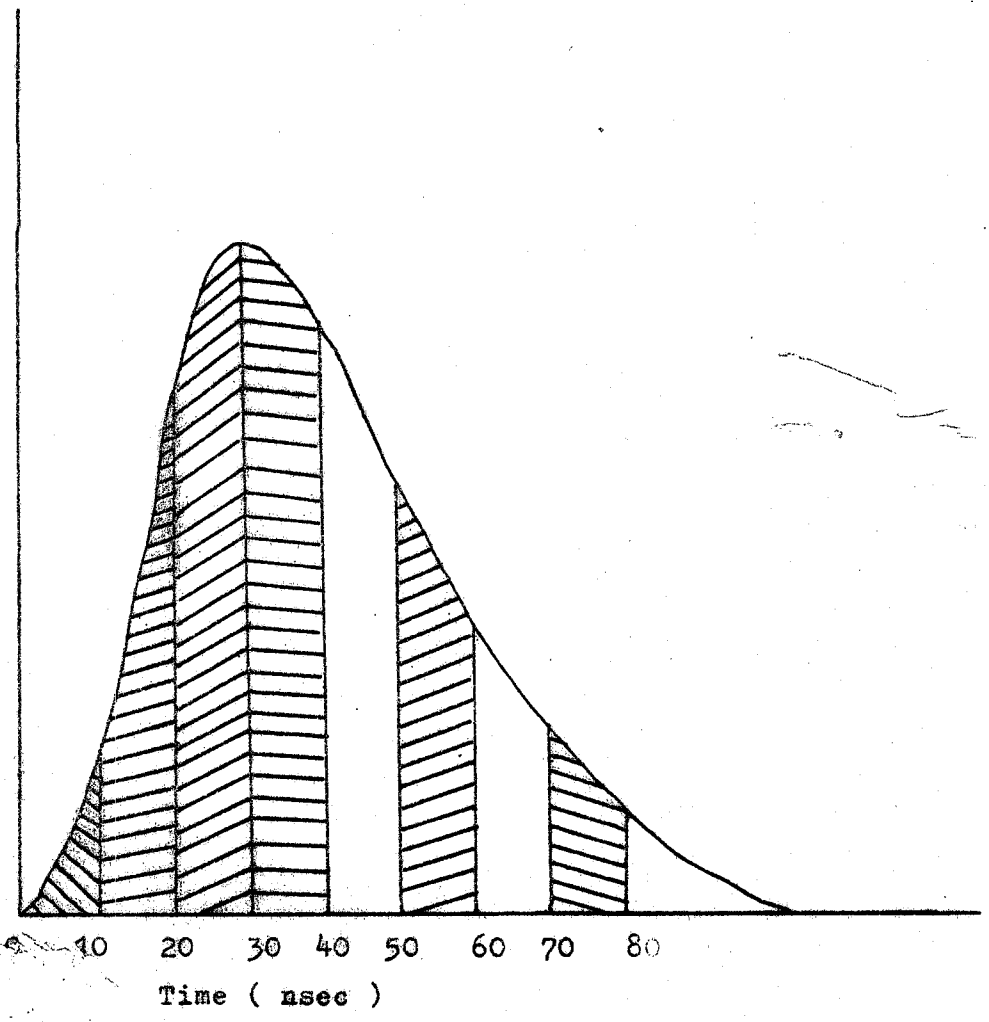
Height
0
10
20
30
40
50
60
70
80
Time (nsec)

and time of arrival to determine the lateral distribution and arrival direction of the light. By reconstructing the pulse using the slice information it would be possible to carry out an analysis of the form described in section 2.4 above.

5.3 The Array

5.3.1 The Geometrical layout

All previous measurements of Cerenkov light by the Durham University group were made at Haverah Park. The geometry of this array, which was dictated by the position of existing facilities and was shown in figure 2-3. Figure 5-2 shows the layout for the new experiment. The main difference being the outer detectors which have been moved in by 100 metres from 500 to 400 metres and then rotated through 60 degrees with respect to the inner ring of detectors. The reason for this change being that after studying the response of various array shapes to a likely flux of showers, it was found that this shape would have the greatest number of 7 fold responses with core distances up to 700 metres for showers of energy 3.10^{17} eV, (Orford 1977 , private communication). As well as this increased response, an array of this shape, from simple considerations, facilitates a more rigorous determination of the radius of curvature of the shower fronts. If the fronts are spherical, which to the experimental accuracy of previous experiments they have been found to be, then the arrangements of the detectors is an important consideration in the degree of non-sphericity which can be observed. If the local zenith angle as determined by groups of three detectors are used to

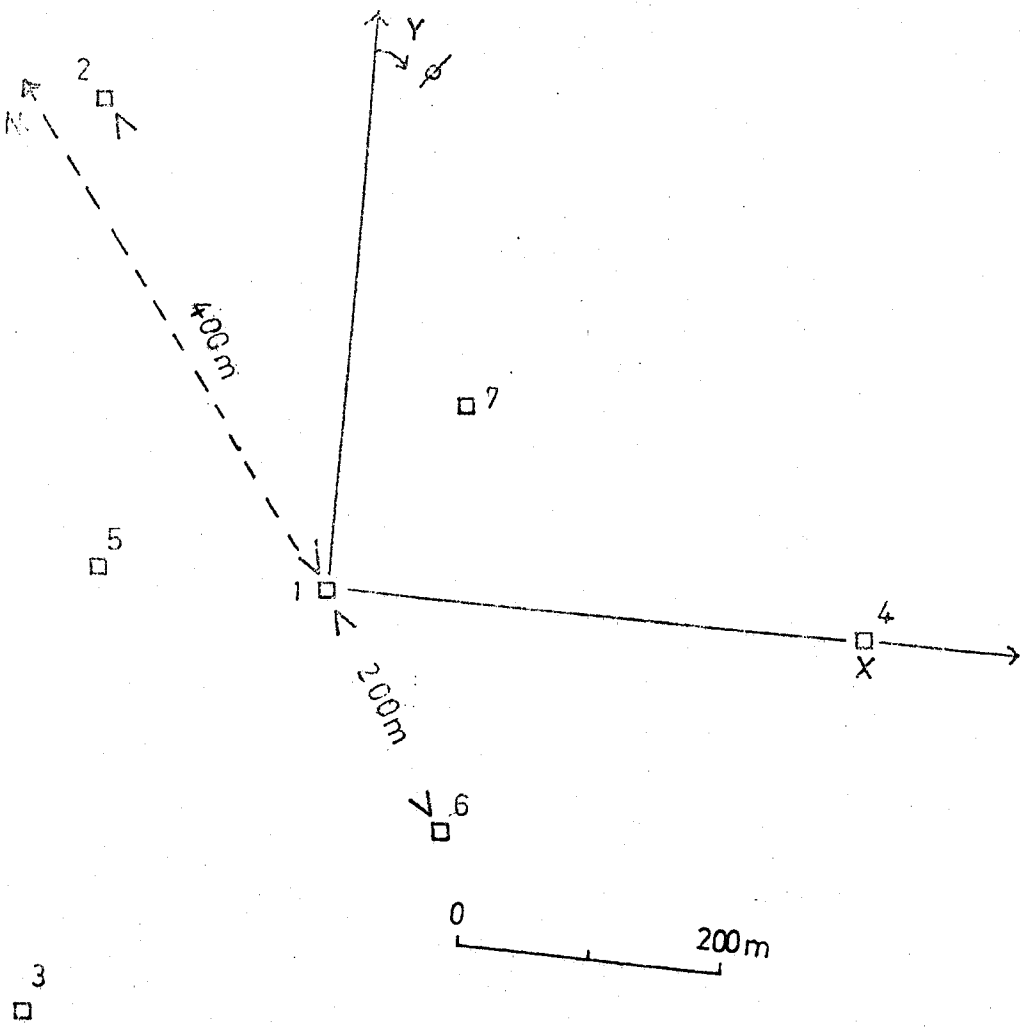
Y
2
400m
7
5
1
4
X
200m
6
0
200m
3

determine shower direction and curvature then it is clear that each group of three must define the vertices of equilateral triangles for all the projected directions to coincide. Figure 5-3 shows the situation schematically for 2 dimensions, where the inferred directions are projected to define the origin of the light front. From this consideration, it was thought that for other techniques of arrival direction and curvature determination, an array composed of interlocking equilateral triangles, as is the new array, would reduce selection effects caused by the radius of curvature being determined from an essentially random set of points. Any non-sphericity would also become more immediately apparent as, for example, a parabolic front would produce a line rather than a point source if triangles of differing sizes were employed.

The projected array will be triggered if a coincidence is found between the centre and any two of the inner ring detectors. This sampling will ensure that most the showers are centrally placed, thus increasing the average number of detectors which show a response to an event.

5.3.2 The Detectors

The detectors used will be similar to those tested at Volcano Ranch, Albuequerque, New Mexico during the winter of 1976. A description of this experiment will be found in Waddoup (1978). The system consists of a photomultiplier, viewing the night sky directly, whose output is digitised in situ and passed to a central recording station in digital form.

The photomultiplier and its electronics are housed in a weather proof aluminium box, which is kept at a constant temperature. A blind covers the photomultiplier during the day to minimise the possible bleaching of the photocathode by exposure to direct sunlight.

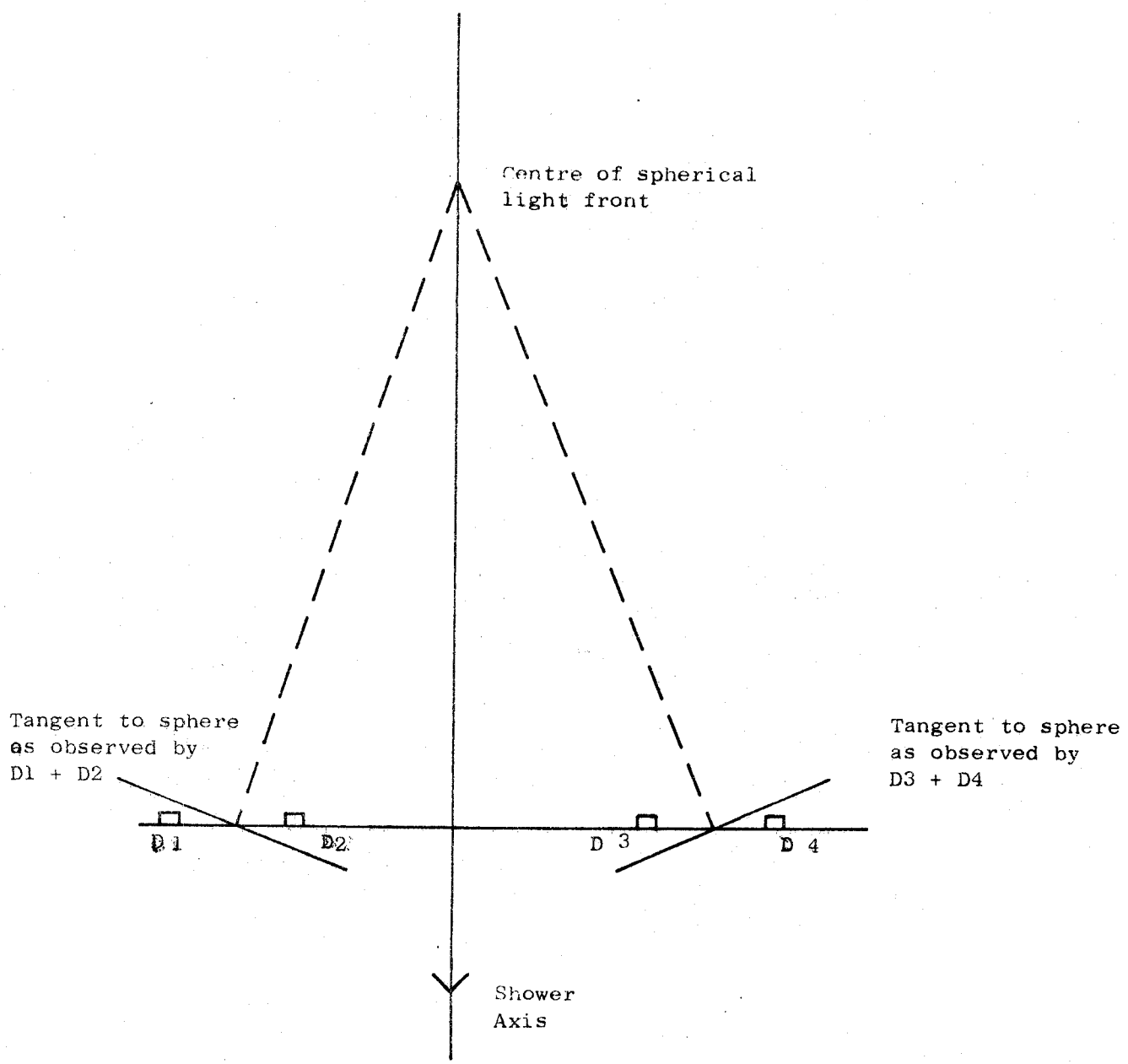
Centre of spherical light front
Tangent to sphere as observed by D1 + D2
Tangent to sphere as observed by D3 + D4
D 1
D2
D 3
D 4
Shower Axis

Similar photomultipliers, RCA 4522's, to those used recently at Haverah Park are employed. However, they are run under slightly different conditions, in that although the interdynode potential will be the same the number of dynodes used is lower, thus reducing the potential of the photocathode. This modification was made to reduce the possible deterioration of the photocathode or dynode resistors noticed during the last two years at Haverah Park. A consequence of this change has been a smaller output pulse, a maximum height of 1 mV is expected. To overcome this the output is amplified by a factor of 100 by a combination of a VV100 (a 100 MHz photomultiplier amplifier from Le Croy Instruments Inc.) and a discrete 100 MHz 10 x amplifier.

Figure 5-4 shows schematically the post-amplication electronics. Firstly the signal coming out of the amplifier is split two ways; one channel going to the discriminator unit, the other to a further fanout stage. The latter produces seven pulses which are used to determine the pulse area and the information on the segments of the pulse.

At the heart of the detector is a seven channel charge to time converter (QTC), which utilizes the hybrid integrated circuit QT 100 B (from Le Croy Inc.). This unit measures the charge on the input during the period of an externally operated gate. The gate pulses are initiated by the discriminator module as soon as the discrimination level is reached. The output from the discriminator is fanned out 6 ways, so that the gates can be operated at different times. By delaying the gates by preset amounts it is possible to analyse each channel at a slightly different time and thereby building up a picture of the pulse. The seventh channel is used to analyse the output from the integrator unit.

The time of arrival will be determined by using a time stretcher, a detailed description of this module can be found in Waddoup and Stubbs (1976). The stretcher will be started by a pulse from the discriminator

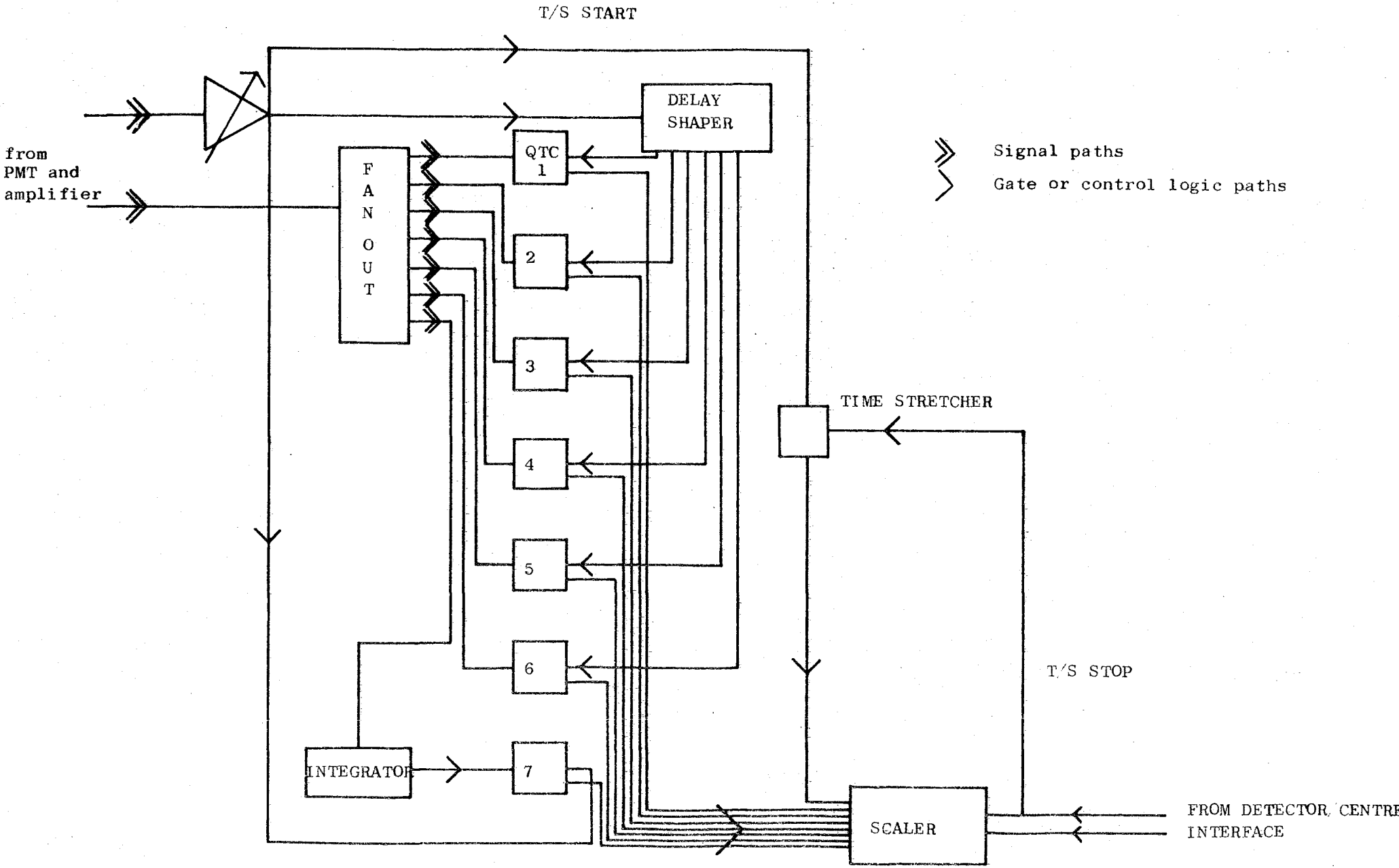
T/S START
DELAY SHAPER
from PMT and amplifier
F A N O U T
QTC 1
2
3
4
5
6
7
INTEGRATOR
TIME STRETCHER
T/S STOP
SCALER
FROM DETECTOR CENTRE INTERFACE
Signal paths
Gate or control logic paths

module at a known time after discrimination, it will be stopped by a pulse from the centre which will be initiated a known time after a shower coincidence is made. The output from this module is a TTL pulse, whose length is a fixed factor times the start - stop time, in this instance, x75. The output from the QTC are TTL pulses whose lengths are proportional to the measured charge. All these outputs will be analysed using a variable rate scale, with maximum rate 20 MHz. The information will be clocked down to the central control facilities by 64 1 millisecond pulses; the information will be stored there on magnetic tape.

The apparatus described above has been calibrated and the following conclusions can be drawn:

(1) The pulse area will be known to 1000 mV nsec.

(11) The within pulse areas will be known to within 80 mV nsec.

(111) The time of arrival will be known to better than 1 nanosecond.

The system will be operated so that the standard light unit (SLU) used at Haverah Park will correspond to about 300 mV nsec, a SLU corresponds to the light output from a radioactive pulser Nel30, 2000 photons. Therefore, these figures can be compared to the present operating specifications of Haverah Park, these can be summarised as:

(1) Pulse area to better than 3SLU's

(11) Within pulse timing to better than 2 nanoseconds

(111) Time of arrival to better than 1 nanosecond

By analysing the pulses in terms of the Nyquist sampling rate it is possible to obtain a maximum frequency which can be used in the Fourier transform of the pulse; a sampling rate of 10 nanoseconds gives a maximum frequency of 50 MHz, this is comparable to the Haverah Park bandwidth. However, it has been found that Cerenkov light pulses can be paramaterised, so that the relationship between the sizes of the relative slices can be used to recreate the Cerenkov light pulse to within 2-3 nanoseconds of its real structure. Thus, although the maximum frequency without prior knowledge,

is 50 MHz ,the pulses can be reconstructed to nanosecond accuracy.

5.3.3 The central recording system

The major departure from the operating philosophy of the present Haverah Park array is that the array will be under computer control. The central recording station will consist of a computer, which logs the data from the detectors as well as monitoring the environmental status of each detector . Also in conjunction with this there are various analogue recorders which monitor, e.g. the night sky brightness and each detector anode current.

After an event the computer initiates a calibration so that any change in gain can be immediately included in the analysis. It then records each detectors temperature and anode current, so that any detector outside of its normal operating condition can be flagged.

Shown in figure 5-5 are the pulses from each detector recorded during the initial running of the array. It was one of the largest showers recorded and it clearly shows the slice information can be used to reconstruct the various pulse profiles. The results of a brief analysis are also shown.

5.4 Future Developments of Measurements of the Separation of the Particle and Light

A single measurment of the time delay between the particle and light fronts will be incorporated into the routine data collection of the new array. Initially, the situation will be similar to the measurements made at Haverah Park, described in Chapter 4. A scintillator will be deployed in the vicinity of the central photomultiplier. The time between the arrival of the two fronts will be measured using a time stretcher, in the same manner as the arrival time of the light is measured. The stretcher will be started by the optical signal and stopped by the scintillator pulse after it has been delayed by a suitable amount.

EVENT 186

X=−34m Y=−141m

$\theta = 29.5^{D}$ $\phi = 255.2^{D}$

$\gamma = -2.45$ $\phi(200) = 45000$ mV nsec

R(10%)=9825m D(10%)=302 grms cm^{-2}

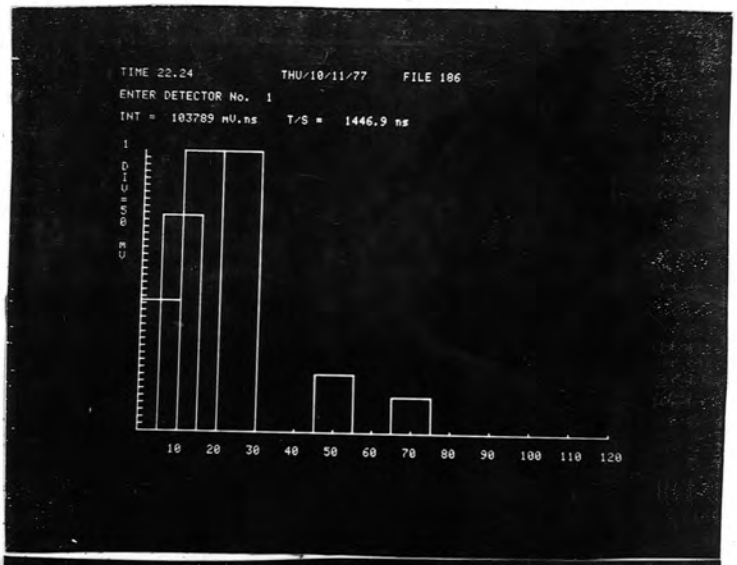

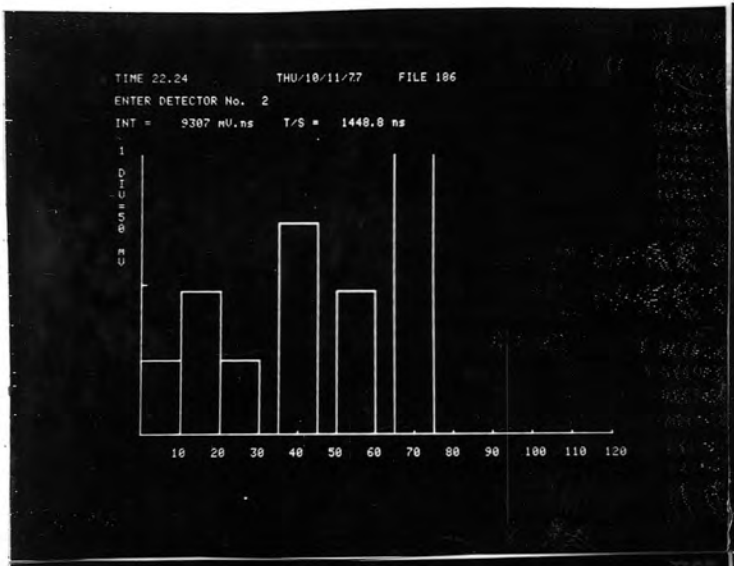

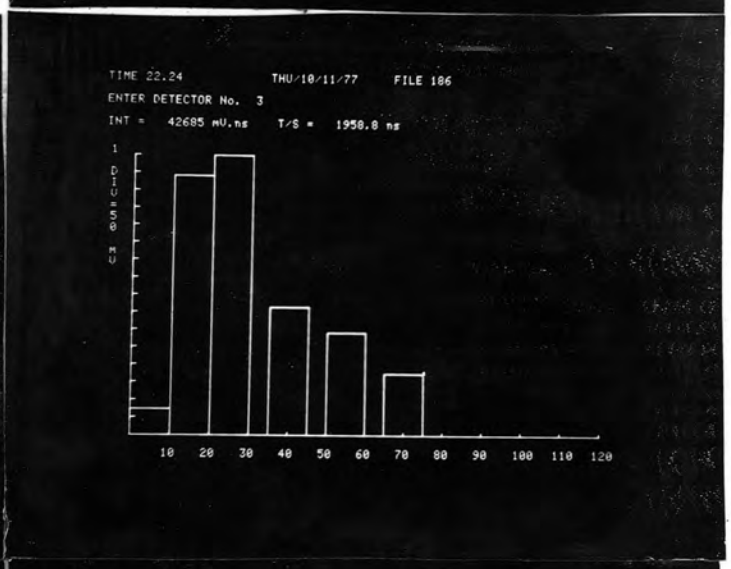

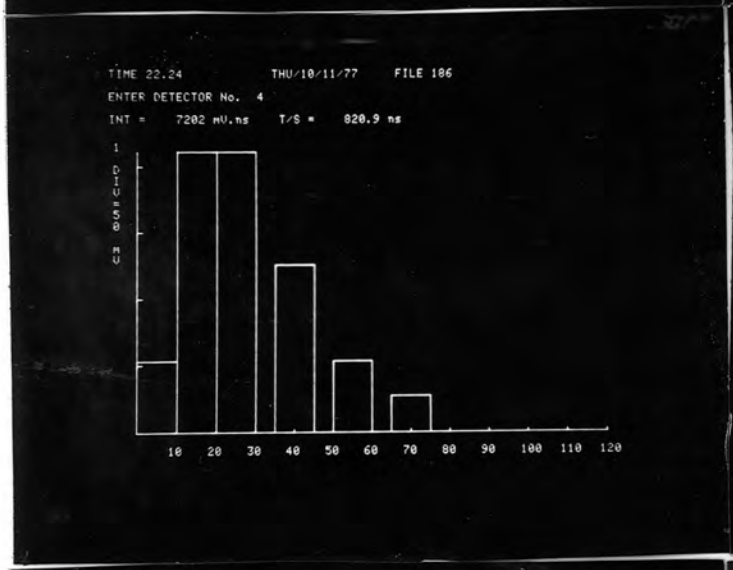

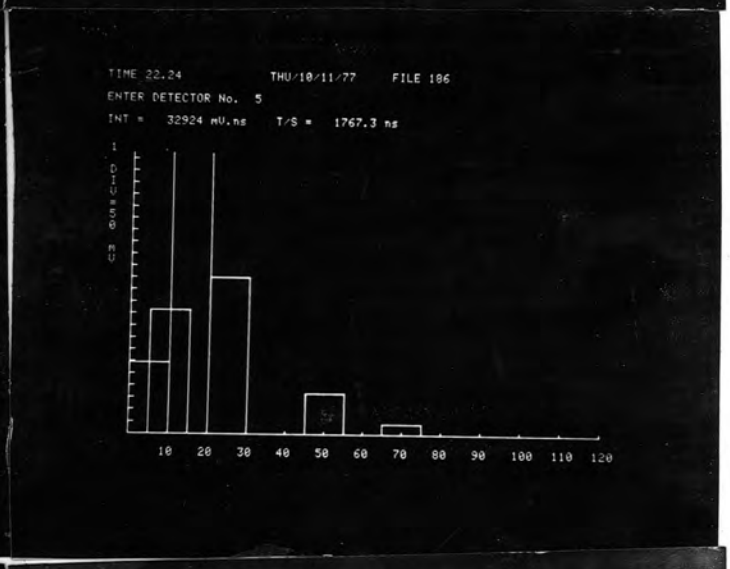

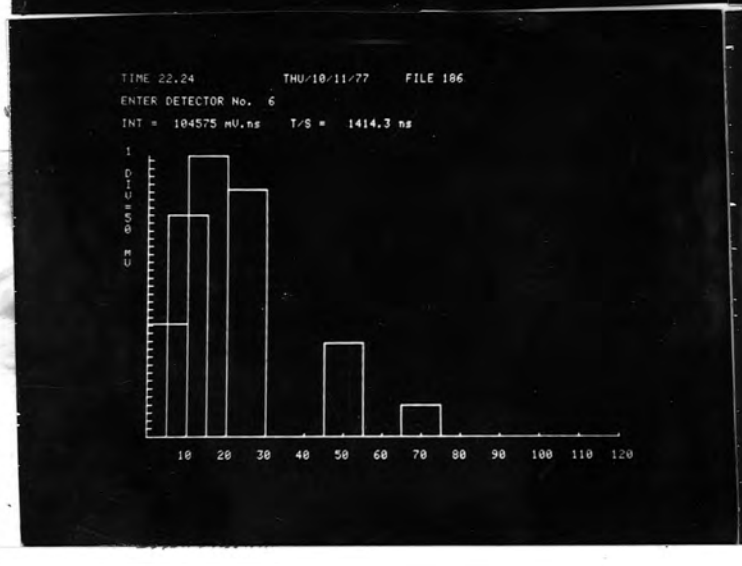

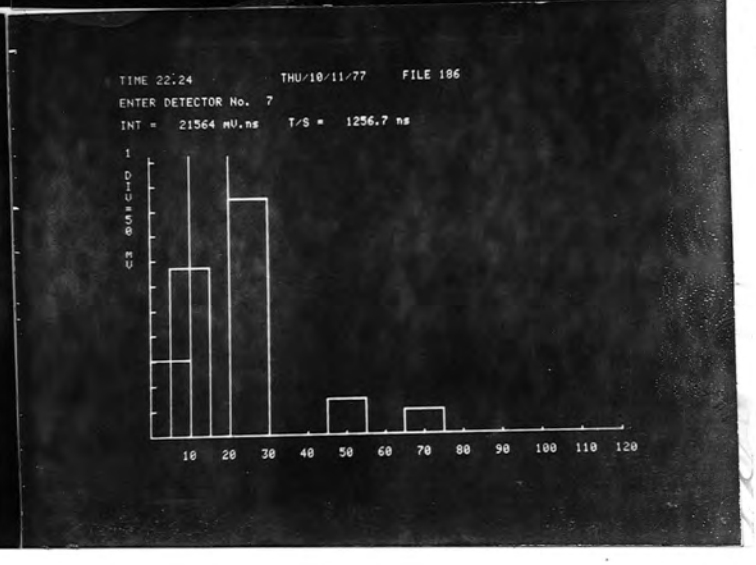

The considerations discussed in the previous chapter concerning the core distance of the scintillator need to be modified for this experiment, as the array will be operated at about 1500 metres above sea level. Here the lateral distribution of electrons will be steeper, so that the core distance at which the small area scintillator can be used may have to be reduced.

It is hoped that later an array of particle detectors will be set up to measure the delay of the particles with respect to the light at various points within the showers. Each will utilise a time stretcher in the same manner described above. The detectors would be most usefully situated with 200 metre optical detectors, although if core distance considerations preclude such a siting, then they could be operated independently with their own photomultipliers. More work will have to be carried out, firstly to understand more fully the response of a single scintillator to a particle flux, and secondly, to develop a better understanding of the relationship between the time separation and a showers development. Although the simulations described in Chapter 3 were adequate to develop this new measurement, they were not sufficiently rigorous to definitely identify the delay with specific aspects of shower development. Further simulations will also have to be carried out to understand the delay higher in the atmosphere.

5.5 Concluding Remarks

The new array will run at a location adjacent to the Fly's Eye experiment described by Beregeson (1975). A combination of the results of these two experiments after a period of simultaneous operation would allow a purely optical multi-parametric analysis of showers to be obtained. As both techniques study the development of the longitudinal cascade directly, it would be possible to determine the depth of Ne maximum to

high precision. Furthermore, the detection of a large number of showers by the Cerenkov array alone, will contribute to the improved understanding of cascade development of showers with primary energy of approximately 10^{17} eV.

Malhotra P.K., Shulka P.G., Stephens S.A., Vijayalakohmi B., Boult J., Bowler M.G., Clapham V.M., Fowler P.H., Hackforth H.L., Keereetareep J. and Tovey S.N., (1966), Nature, 209, 2567.

McCusker, C.B.A., (1967), Proc.10th Int.Conf. in Cosmic Rays, S397.

Nesterova, N.M. and Chudakov A.E. (1955), Zh. Eksp.Teor.Fig., 28, 384.

Orford, K.J. and Turver, K.E. (1976), Nature, 264, 727

Protheroe, R.J. (1978), Ph.D. Thesis, University of Durham.

Protheroe, R.J. and Turver K.E. (1977), Proc.15th Int.Conf. on Cosmic Rays, Plovidiv, 8, 275

Smith, G.J. and Turver K.E. (1973), J.Phys.A, 6, L212.

Tennant, R.M. (196), Proc. Phys. Soc., 92, 622

Waddoup, W.D. (1978), Ph.D. Thesis in preparation.

Waddoup, W.D. and Stubbs R.J. (1976), Nucl.Inst. and Method, 137, 603.

Welby, D.W. (1978), Ph.D. Thesis, University of Durham.

ACKNOWLEDGEMENTS

I am grateful to my supervisor, Dr.K.E.Turver for the initial idea of this thesis and for much encouragement during its completion. I am also indebted to the other members of the Durham University Extensive Air Shower group, namely;

Dr.R.J.Protheroe for a great deal of patience and help with the simulations.

Dr.K.J.Orford for interesting discussions and advice.

Dr.D.W.Welby and Mr.W.D.Waddoup for running the Cerenkov light array during the two seasons of observations.

Mr.R.T.Hammond for useful suggestions on the data analysis.

I am also grateful to Professor A.W.Wolfendale for supplying laboratory facilities during this study. Also, to Neil Verow of the Northumbrian Graphical and Cartoon Cooperative for graphical assistance.

The University of Leeds group are also thanked for the particle data analysis.